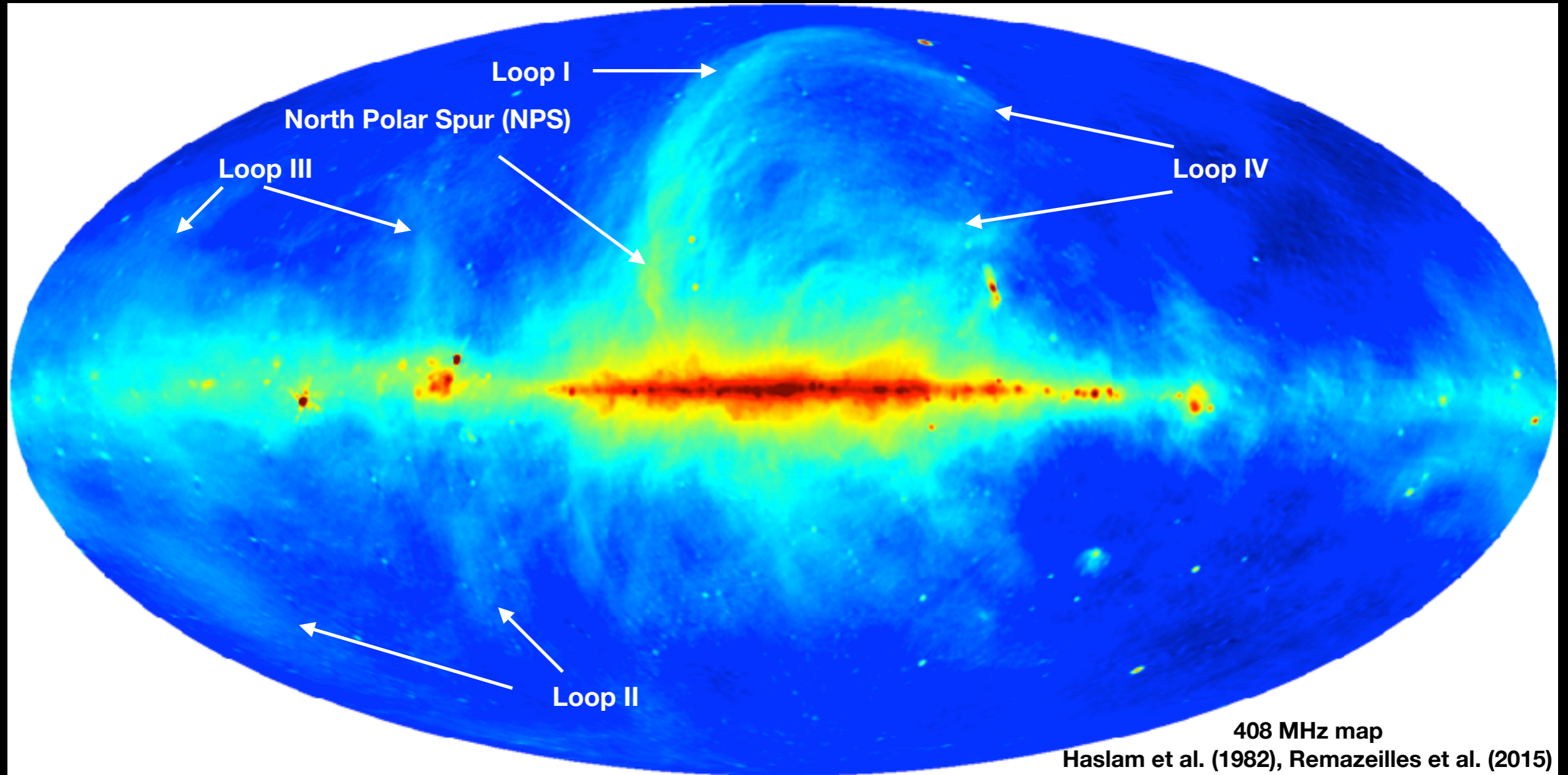


Overview of large-scale features in the radio sky



Prof Clive Dickinson

Jodrell Bank Centre for Astrophysics
School of Physics and Astronomy

The University of Manchester

Three elephants in the gamma-ray sky: Loop I, the Fermi bubbles, and the Galactic Centre excess,
21-24 October 2017, Garmisch-Partenkirchen, Germany

Outline of talk

After brief introduction, mostly material from these 2 papers

(get much clearer view of loops/spurs in polarization - to some degree!)

Monthly Notices

ROYAL ASTRONOMICAL SOCIETY

MNRAS 000, 000–000 (2015)

doi:10.1093/mnras/stv1328

Polarized radio filaments outside the Galactic plane

Matias Vidal,^{*} C. Dickinson, R. D. Davies and J. P. Leahy

Jodrell Bank Centre for Astrophysics, Alan Turing Building, School of Physics and Astronomy, The University of Manchester, Oxford Road, Manchester M13 9PL, UK

Accepted 2015 June 12; Received 2015 June 9; in original form 2014 October 16

ABSTRACT

We used data from the *WMAP* satellite at 23, 33 and 41 GHz to study the diffuse polarized emission over the entire sky. The emission originates mostly from filamentary structures with well-ordered magnetic fields. Some of these structures have been known for decades in radio continuum maps. Their origin is not clear and there are many filaments that are visible for the first time. We have identified and studied 11 filaments. The polarization fraction of some of them can be as high as 40 per cent, which is a signature of a well-ordered magnetic field. The polarization spectral indices, averaged over 18 regions in the sky is $\beta = -3.06 \pm 0.02$, consistent with synchrotron radiation. There are significant variations in β over the sky ($\Delta\beta \approx 0.2$). We explore the link between the large-scale filaments and the local interstellar medium, using the model of an expanding shell in the solar vicinity. We compared observed polarization angles with the predictions from the model and found good agreement. This strongly suggests that many large-scale filaments and loops are nearby structures. This is important in the context of the Galactic magnetic field as these structures are normally included in global models, neglecting the fact that they might be local. We also studied the level of contamination added by the diffuse filaments to the CMB (cosmic microwave background) polarization power spectra. We conclude that, even though these filaments present low radio brightness, a careful removal will be necessary for future all-sky CMB polarization analysis.

Key words: polarization – radiation mechanisms: general – radiation mechanisms: non-thermal – ISM: magnetic fields – diffuse radiation – radio continuum: ISM.

A&A 594, A25 (2016)
DOI: 10.1051/0004-6361/201526803
© ESO 2016

Planck 2015 results

Planck 2015 results

XXV. Diffuse low-frequency Galactic foregrounds

Planck Collaboration: P. A. R. Ade²⁵, N. Aghanim⁶⁴, M. I. R. Alves^{115,116}, M. Arnaud⁷², M. Ashikhmin^{72,5}, J. Aumont⁶⁴, C. Baccigalupi³⁰, A. J. Banday^{102,11}, R. B. Barreiro³⁰, J. G. Bartlett¹⁷², N. Bartolo^{23,71}, F. Battaner^{107,108}, K. Benabib^{22,104}, A. Bernini⁵², A. Bersani-Lévy^{27,65,104}, J.-P. Bernard^{125,11}, M. Bersanelli^{33,22}, P. Bielewicz^{39,11,92}, J. J. Bock^{32,15}, A. Bonaldi³³, L. Bonavera³⁰, J. R. Bond¹², J. Borrill^{15,59}, F. R. Bouchet^{65,9}, F. Boulanger⁶⁴, M. Bucher¹, C. Burigana^{51,54,53}, R. C. Butler⁵, E. Calabrese¹²¹, J.-F. Cardoso^{21,1,65}, A. Catalanu^{81,78}, A. Challinor^{57,75,14}, A. Chamballu^{29,14,64}, R.-R. Chary⁶¹, H. C. Chiang^{30,7}, P. R. Christensen^{60,74}, S. Colombi^{65,104}, L. P. L. Colombo^{30,77}, C. Combet⁸¹, F. Couchot⁷⁷, A. Coulais³⁸, B. P. Crill^{72,12}, A. Curio^{10,6,75}, F. Cuttaia⁵¹, L. Danese³⁰, R. D. Davies¹², R. J. Davis¹², P. de Bernardis³⁰, A. de Rosa¹¹, G. de Zotti^{18,95}, J. Delabrouille¹, J.-M. Delon^{65,101}, H.-X. Döser⁷⁸, C. Dickinson^{73,7}, J. M. Diego³⁰, H. Dole^{10,65}, S. Donzell⁶⁵, O. Doré^{75,15}, M. Doustpis⁶⁴, A. Ducour^{65,53}, X. Dupac¹¹, G. Efstathiou³⁷, F. Elsner^{27,65,101}, T. A. Enßlin³⁵, H. K. Eriksen⁶⁴, E. Falgarone⁷⁴, J. Fergussan¹⁴, F. Finelli^{51,53}, O. Forti^{105,11}, M. Frailis⁹¹, A. A. Fraisse³⁰, E. Franceschi³¹, A. Freijsel³⁰, S. Galeotta³¹, S. Galli⁷⁵, K. Ganga¹, T. Ghosh⁶⁴, M. Giardi^{122,11}, Y. Giraud-Héraud¹, E. Gjerløw²⁴, J. González-Nuevo^{22,21}, K. M. Górski^{72,110}, S. Gratton^{72,67}, A. Gregorio^{27,51,57}, A. Gruppene⁵¹, J. E. Gudmundsson^{122,21,30}, F. K. Hansen⁶⁸, D. Hanson^{31,72,10}, D. L. Harrison^{61,75}, G. Heiles¹³, S. Henric-Olsen¹²⁷, C. Hernández-Monteagudo^{12,52}, D. Herranz²⁹, S. R. Hildebrandt^{72,12}, E. Hivon^{22,104}, M. Hobson⁷², W. A. Holmes⁷², A. Hornstrup¹², W. Howett¹², K. M. Huffenberger¹⁴, G. Hurier²⁴, A. H. Jaffe⁶⁹, T. R. Jaffe^{105,11}, W. C. Jones³⁶, M. Juvela²², F. Keihänen²², R. Keskitalo¹⁵, T. S. Kisner²⁵, R. Kneissl^{40,3}, J. Knoche²⁰, M. Kunz^{10,65,3}, H. Kurki-Suonio^{29,42}, G. Lagache^{3,64}, A. Lähteenmäki^{12,46}, J.-M. Lamarre²³, A. Lasenby^{15,53}, M. Lattanzi^{35,53}, C. R. Lawrence²², J. P. Leahy^{73,7}, R. Leonardi¹, J. Lesgourgues^{105,104}, F. Levrier¹⁸, M. Liguori^{31,71}, P. B. Lilje⁶, M. Linden-Vørnle¹⁰, M. López-Cañiego^{71,72}, P. M. Lubin¹¹, J. P. Mielas-Pérez¹¹, G. Maggio³¹, D. Maino^{15,52}, N. Mandolese^{51,34}, A. Mangilli^{24,77}, M. Maris³¹, D. J. Marshall¹², P. G. Martin¹⁰, E. Martínez-González³¹, S. Masi⁷⁵, S. Matarrese^{27,71,47}, P. McGhee²³, P. K. Meindhördt¹, A. Melchiorri^{22,22}, L. Mendes⁶¹, A. Mennella^{22,22}, M. Migliaccio^{67,72}, S. Mitra^{23,72}, M.-A. Miville-Deschênes^{64,10}, A. Moneti⁶⁷, L. Montier^{106,11}, G. Morgante⁷¹, D. Mortlock⁴⁶, A. Moss¹⁵, D. Munshi¹⁵, J. A. Murphy³⁴, F. Natali³, F. Nati^{34,53}, C. B. Netterfield²⁷, H. U. Nørgaard-Nielsen¹⁵, F. Novello⁷³, D. Novikov^{27,24}, I. Novikov^{27,24}, E. Orlando¹⁰⁶, C. A. Oxborrow¹², F. Pacif¹², L. Pagani^{25,55}, F. Pajot⁶⁴, R. Paladini⁹¹, D. Panfili^{21,22}, B. Partridge⁴⁸, F. Pasian²², G. Patanchon¹, T. J. Pearson^{12,51}, M. Peel⁷², O. Perdereau⁷⁷, L. Perotto⁸¹, F. Perrotta³⁰, V. Pettorino⁴⁴, F. Piacentini²⁵, M. Piat¹, E. Pierpaoli²⁴, D. Pierobon⁷², S. Planck Collaboration^{105,11}, G. Polenta^{1,69}, G. W. Pratt¹⁹, G. Prézeau^{13,72}, S. Prunet^{65,105}, J.-L. Puget⁶¹, J. P. Rachen^{27,105}, W. T. Reach¹⁰, R. Rebolo^{15,17,21}, M. Reinecke⁸², M. Remazeilles^{11,65,1}, C. Renaud¹, A. Renzi^{18,25}, I. Ristorcelli^{105,11}, G. Rocha^{27,13}, C. Rosseti^{105,52}, G. Roudier^{1,35,75}, J. A. Rubiño-Martín^{60,71}, B. Rusholme⁶¹, M. Sandri⁷, D. Santos⁶¹, M. Savolainen^{24,45}, G. Savini⁷², D. Scott⁷⁴, M. D. Seiffert^{72,17}, E. P. S. Shellard¹, L. D. Spencer⁶⁵, V. Stolyarov^{61,71,5}, R. Stompar¹, A. W. Strong²⁵, R. Sudwala⁶⁷, K. Sunyaev^{65,68}, D. Sutton^{67,75}, A.-S. Suur-Uusi^{28,46}, J.-F. Sygnet⁶⁷, J. A. Tauber⁷², L. Terenzi^{105,51}, L. Toffolatti^{75,31,51}, M. Tomasi^{35,72}, M. Tristram⁷⁷, M. Tucci¹², J. Tuovinen¹², G. Umata⁶⁷, I. Valenziano¹, J. Valiviita^{24,46}, F. Van Tent²², M. Vidal⁷³, P. Vielva⁷³, F. Villa¹¹, I. A. Wade⁷², B. D. Wandelt^{67,106,72}, R. Watson⁷³, I. K. Wehus^{72,65}, A. Wilkinson⁷², D. Yvon¹⁸, A. Zaccari²⁰, and A. Zonca²¹

(Affiliations can be found after the references)

Received 22 June 2015 / Accepted 20 April 2016

ABSTRACT

We discuss the Galactic foreground emission between 20 and 100 GHz based on observations by *Planck* and *WMAP*. The total intensity in this part of the spectrum is dominated by free-free and spinning dust emission, whereas the polarized intensity is dominated by synchrotron emission. The *Commander* component-separation tool has been used to separate the various astrophysical processes in total intensity. Comparison with radio recombination line templates verifies the recovery of the free-free emission along the Galactic plane. Comparison of the high-latitude H α emission with our free-free map shows residuals that correlate with dust optical depth, consistent with a fraction ($\approx 50\%$) of H α having been scattered by high-latitude dust. We highlight a number of diffuse spinning dust morphological features at high latitude. There is substantial spatial variation in the spinning dust spectrum, with the emission peak (in I_{ν}) ranging from below 20 GHz to more than 50 GHz. There is a strong tendency for the spinning dust component near many prominent H II regions to have a higher peak frequency, suggesting that this increase in peak frequency is associated with dust in the photo-dissociation regions around the nebulae. The emissivity of spinning dust in these diffuse regions is of the same order as previous detections in the literature. Over the entire sky, the *Commander* solution finds more anomalous microwave emission (AME) than the *WMAP* component maps, at the expense of synchrotron and free-free emission. This can be explained by the difficulty in separating multiple broadband components with a limited number of frequency maps. Future surveys, particularly at 5–20 GHz, will greatly improve the separation by constraining the synchrotron spectrum. We combine *Planck* and *WMAP* data to make the highest signal-to-noise ratio maps yet of the intensity of the all-sky polarized synchrotron emission at frequencies above a few GHz. Most of the high-latitude polarized emission is associated with distinct large-scale loops and spurs, and we re-discuss their structure. We argue that nearly all the emission at $40^{\circ} < l < 90^{\circ}$ is part of the Loop I structure, and show that the emission extends much further in to the southern Galactic hemisphere than previously recognised, giving Loop I an ovoid rather than circular outline. However, it does not continue as far as the “*Fermi* bubble/microwave haze”, making it less probable that these are part of the same structure. We identify a number of new faint features in the polarized sky, including a dearth of polarized synchrotron emission directly correlated with a narrow, roughly $20'$ long filament seen in H α at high Galactic latitude. Finally, we look for evidence of polarized AME, however many AME regions are significantly contaminated by polarized synchrotron emission, and we find a 2σ upper limit of 1.6% in the Perseus region.

Key words. diffuse radiation – ISM: general – radiation mechanisms: general – radio continuum: ISM – polarization – local interstellar matter

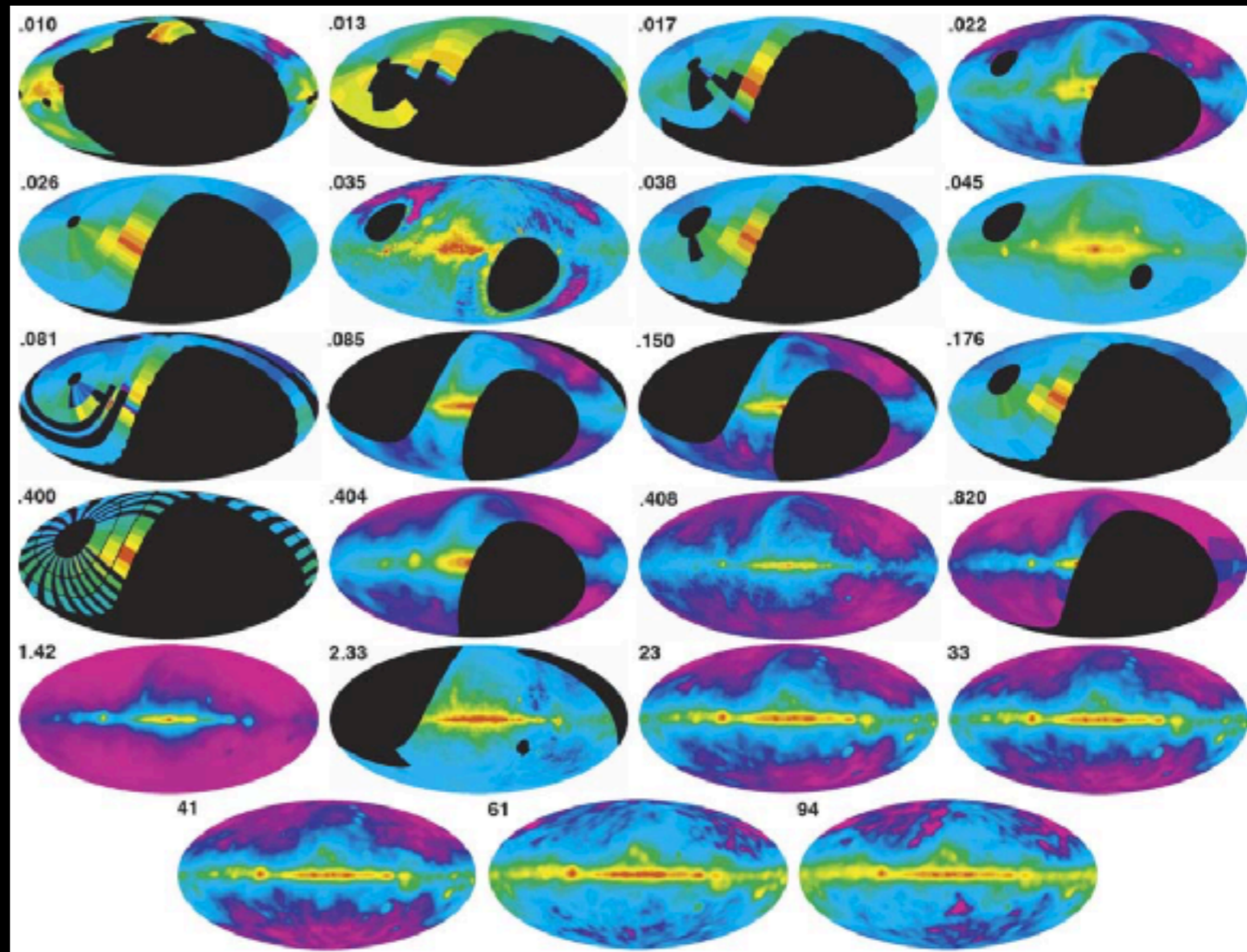
* Corresponding authors: C. Dickinson, c11ve.dickinson@manchester.ac.uk; J. P. Leahy, j.p.leahy@manchester.ac.uk

Radio emission mechanisms (overview)

Emission Mechanism	Description	Typical spectrum	Polarisation
Synchrotron radiation	Electrons accelerated in magnetic field	Curved power-law -2.7 (optically thin above ~ 100 MHz)	Up to $\sim 70\%$
Free-free radiation	Electrons accelerated by ions	Power-law -2.1 (optically thin above $\sim 100+$ MHz)	~ 0
Anomalous Microwave Emission (AME) - electric dipole radiation	Electric dipoles of small spinning dust grains	Peaked spectrum $\sim 10-100$ GHz Peak ~ 30 GHz (?)	~ 0
Cosmic Microwave Background (CMB)	Blackbody radiation	Blackbody ($T=2.726$ K) Peaks ~ 200 GHz	$\sim 10\%$
Magnetic dipole radiation	Magnetic dipole from thermal fluctuations of magnetization	\sim Blackbody emitting in microwave/sub-mm. Complicated in polarisation (varied)	Up to $\sim 30\%$

Large-scale radio surveys

- Few attempts so far!
 - Interferometers no good - no sensitivity to large scales
- Large-scale mapping very difficult!
 - Gain fluctuations (1/f noise)
 - Atmospheric fluctuations
 - Ground-spillover
 - Large beams (source contamination)
 - Absolute calibration very difficult!
 - “Older” surveys particularly vulnerable to systematic errors/poor calibration
- Fewer surveys in polarisation!
 - Faraday Rotation below ~ 3 GHz
 - WMAP/Planck give high frequency (20-100 GHz) view with high S/N and full-sky polarisation



de Oliveira-Costa et al. (2008)

Early radio maps

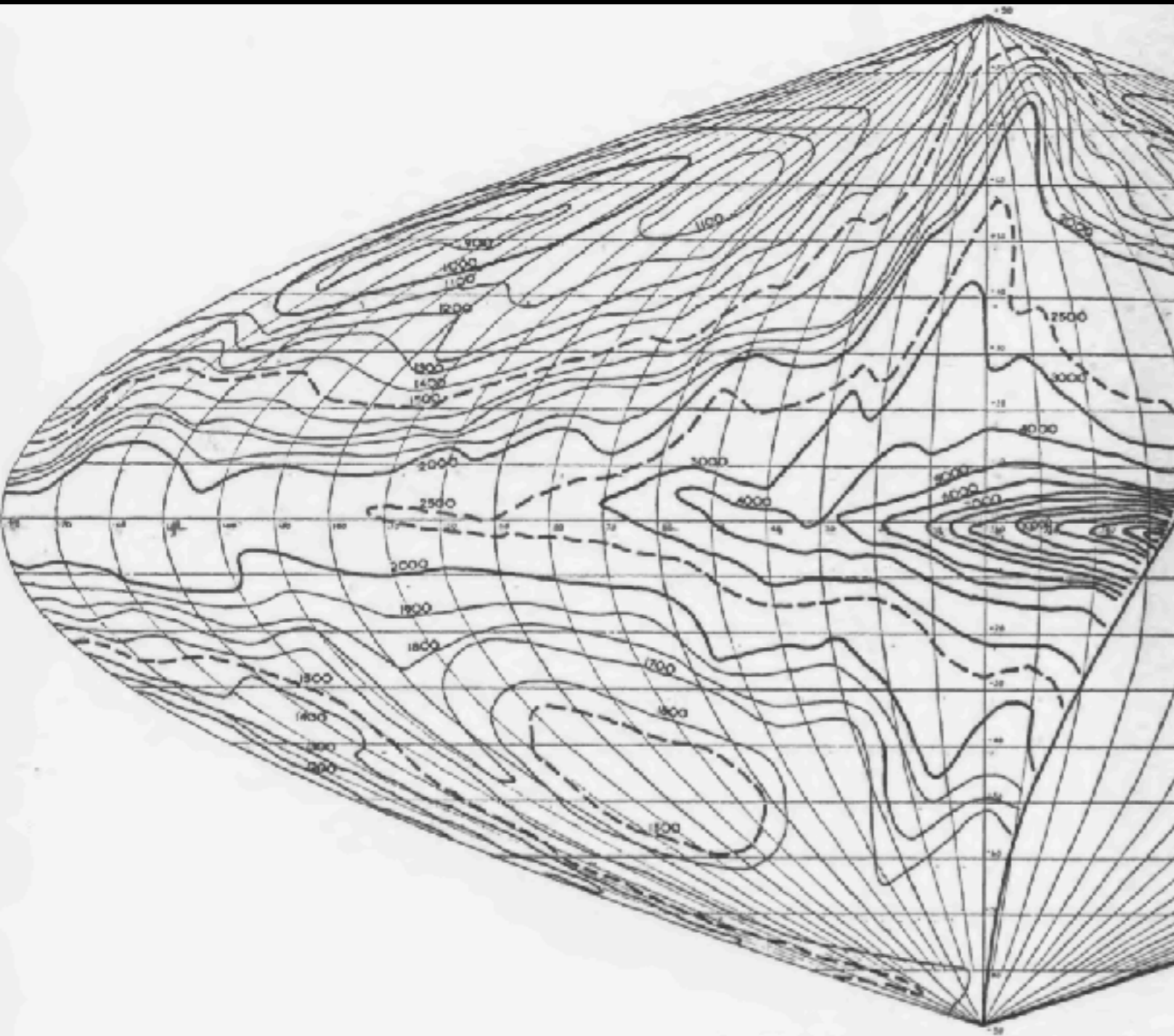


FIG. 4.—Map of the integrated radiation in galactic coordinates.
— intervals of 100 deg. K
- - - intervals of 500 deg. K
— intervals of 1000 deg. K.

81.5 MHz (Baldwin et al. 1955)

Loop I discovered by Bolton & Westfold (1950)
but visible in Jansky's 1935 data! (O'Sullivan book)



160 MHz (Reber et al. 1944)

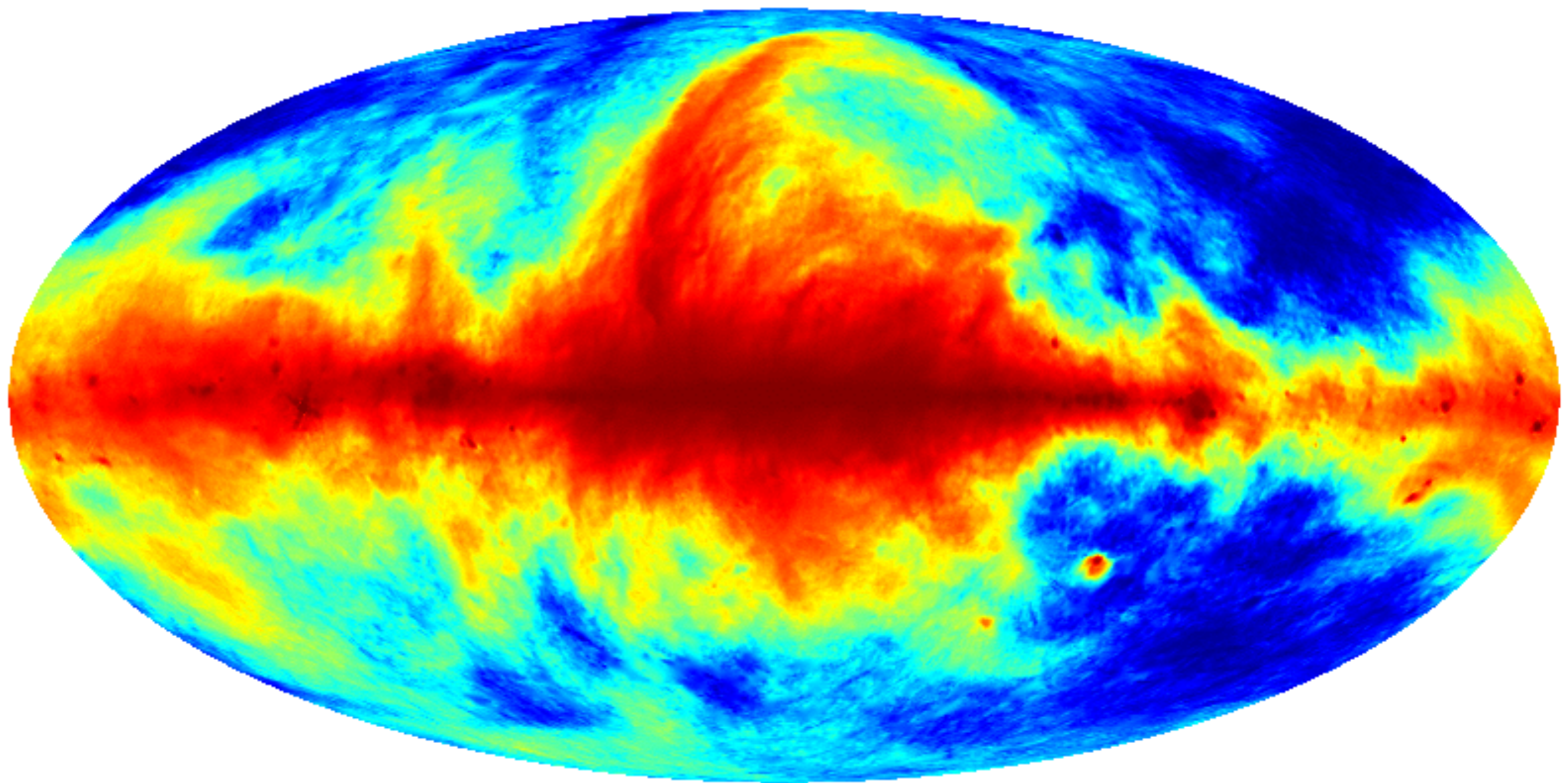
First map of the radio sky as produced by Grote Reber showing strong sources of radiation in Cassiopeia, in Cygnus and in Sagittarius, the center of the galaxy, the region from which Karl Jansky had detected radio emission.

Improved all-sky 408 MHz map

Haslam et al. (1981, 1982) -> Bennett et al. (2003) “Lambda” version

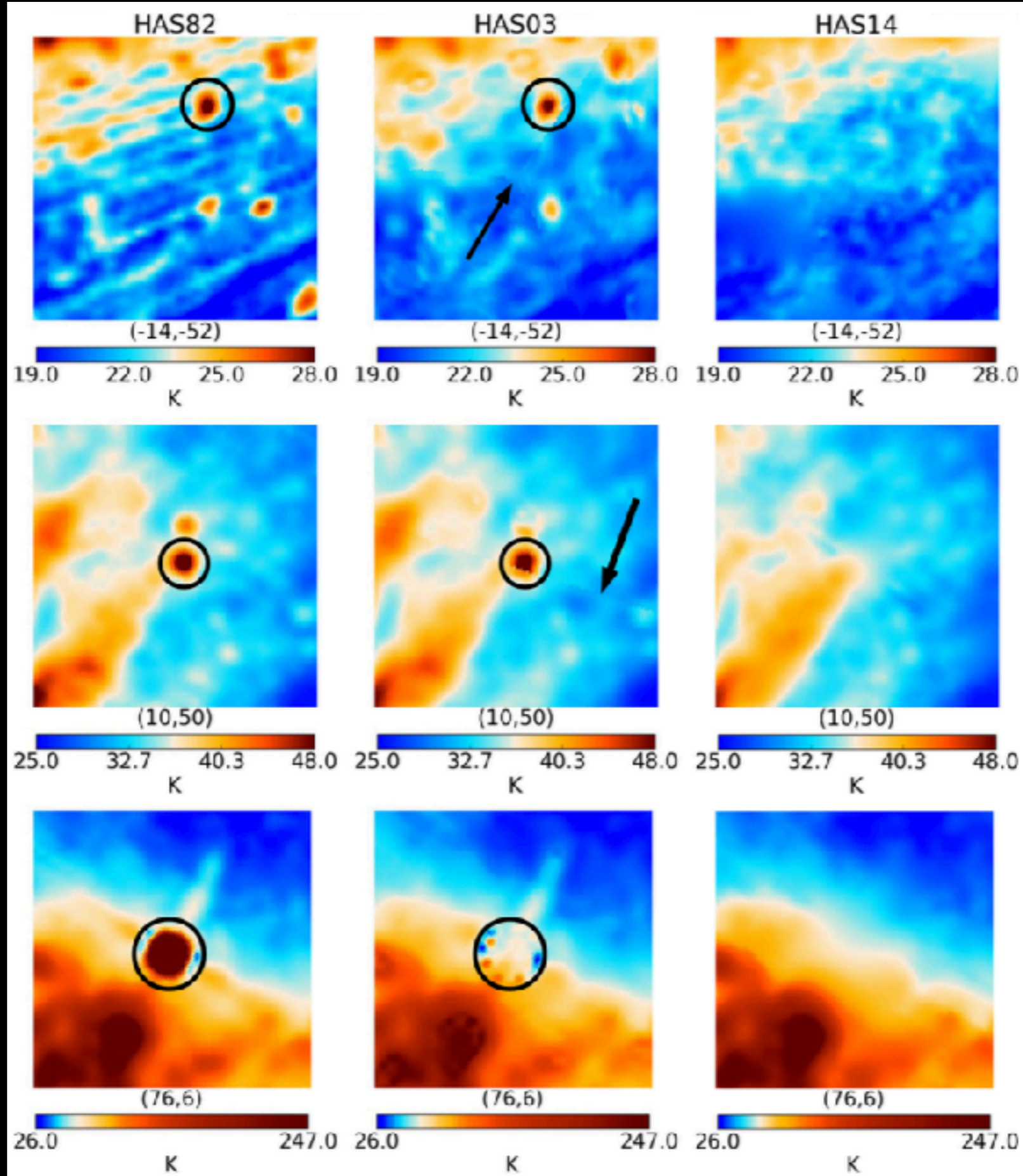
-> **Remazeilles et al. (2015) version**

(better source removal, destriping, matching of surveys, quantification of main beam etc.)
(still many artifacts though!)



Improved all-sky 408 MHz map

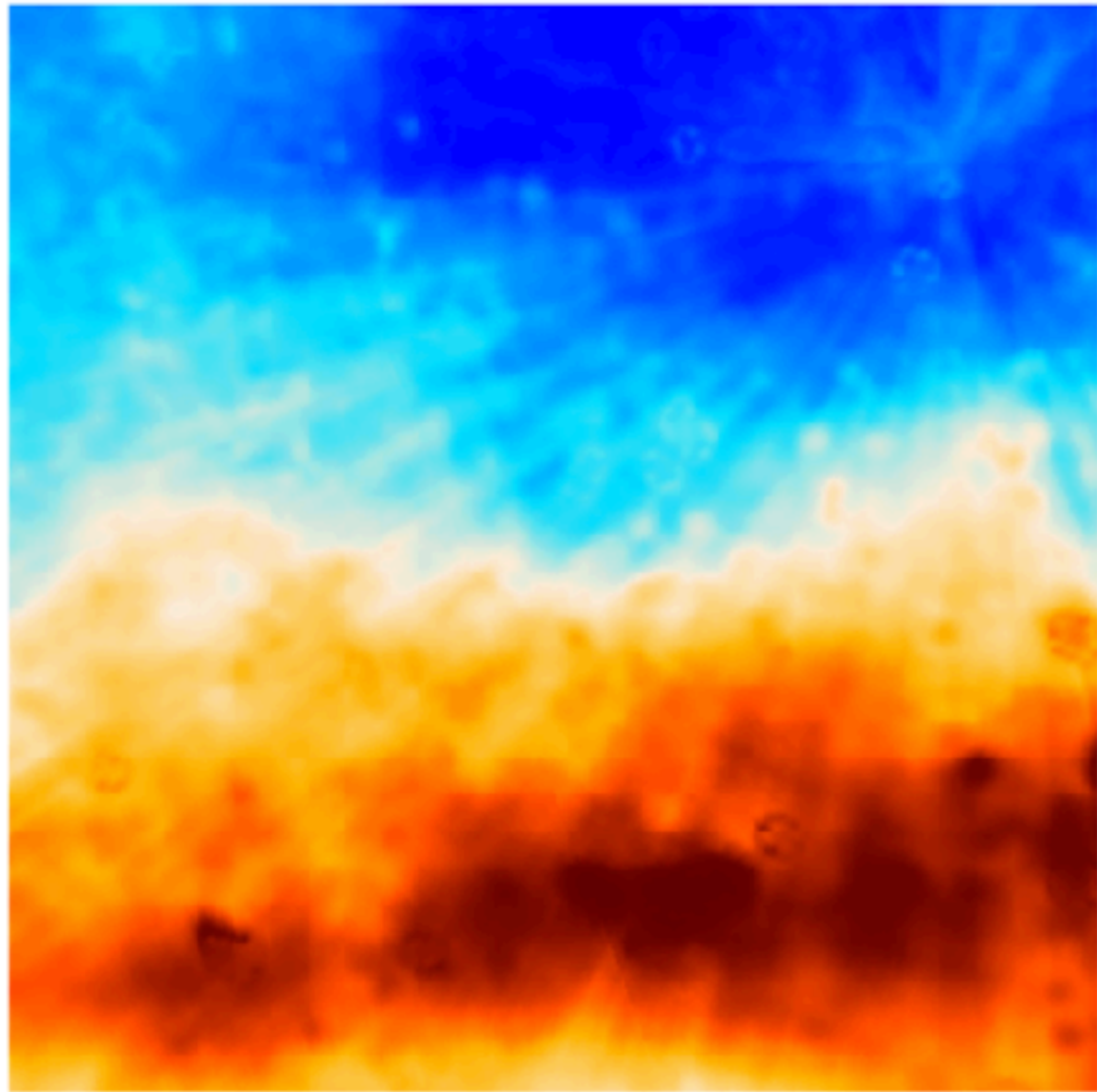
Remazeilles et al. (2015)



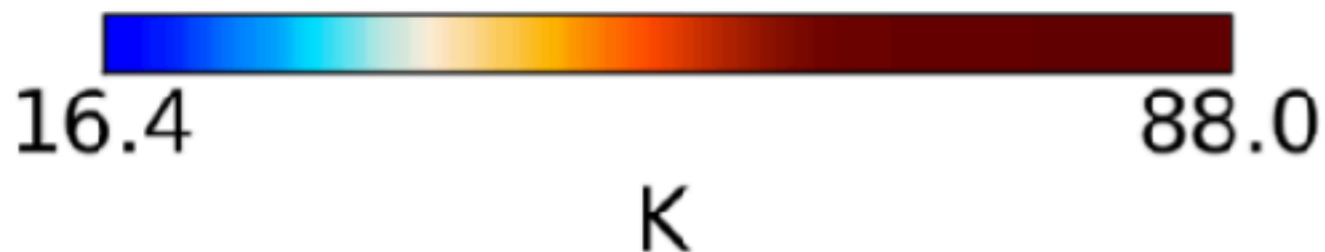
Improved all-sky 408 MHz map

Remazeilles et al. (2015)

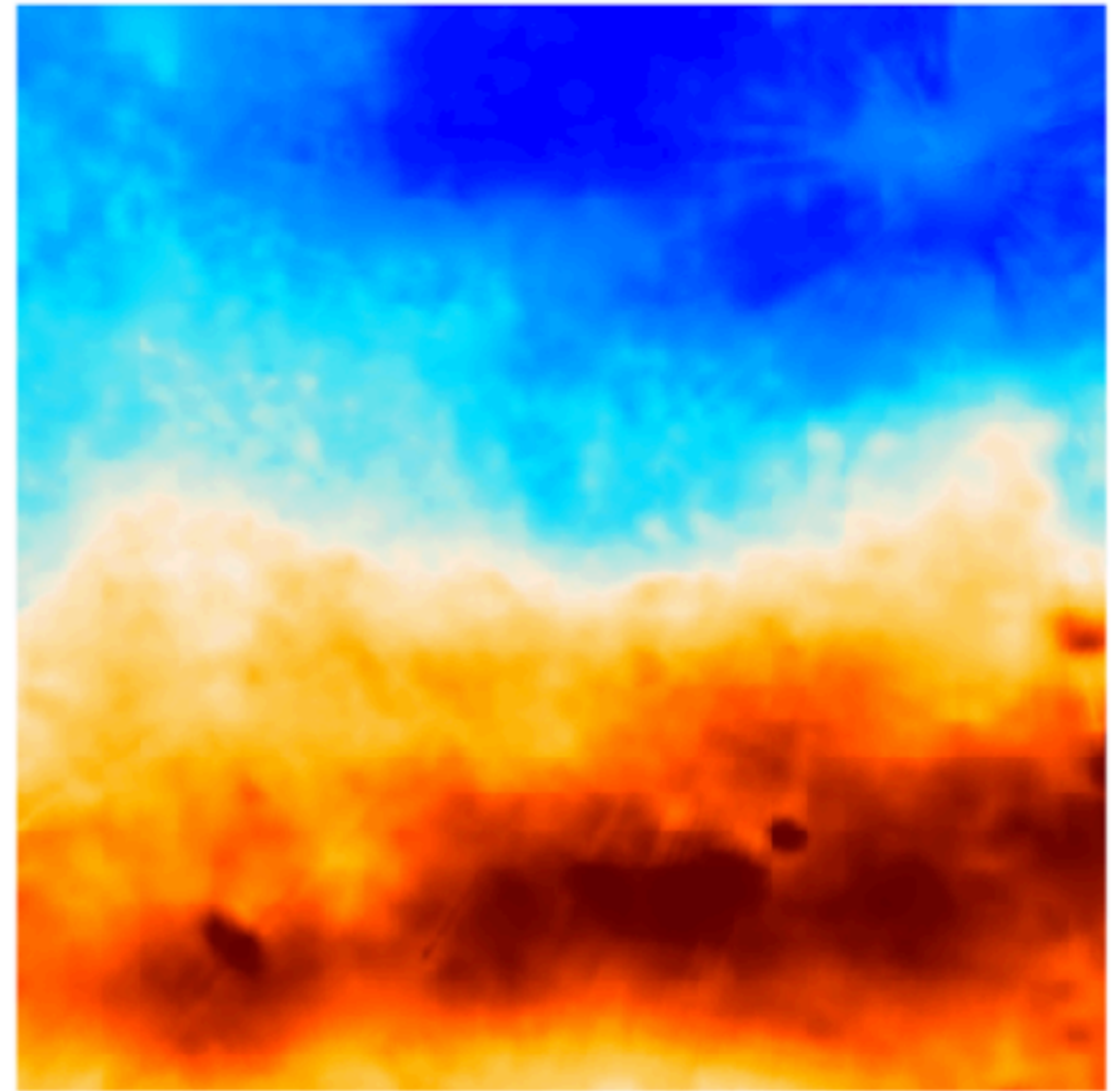
HAS03



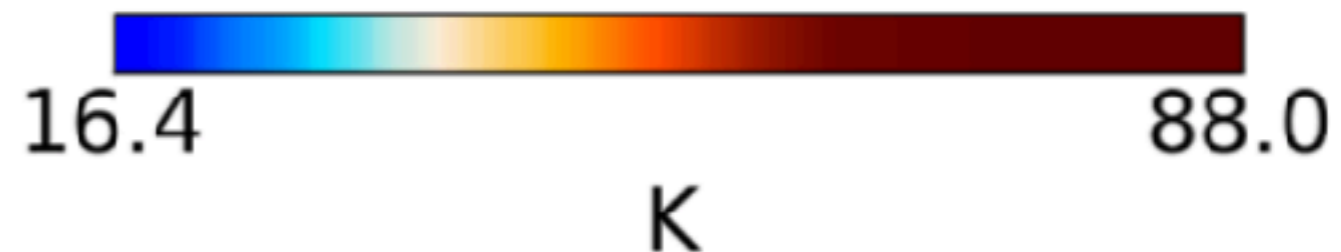
(139.1, 14.0)



HAS14

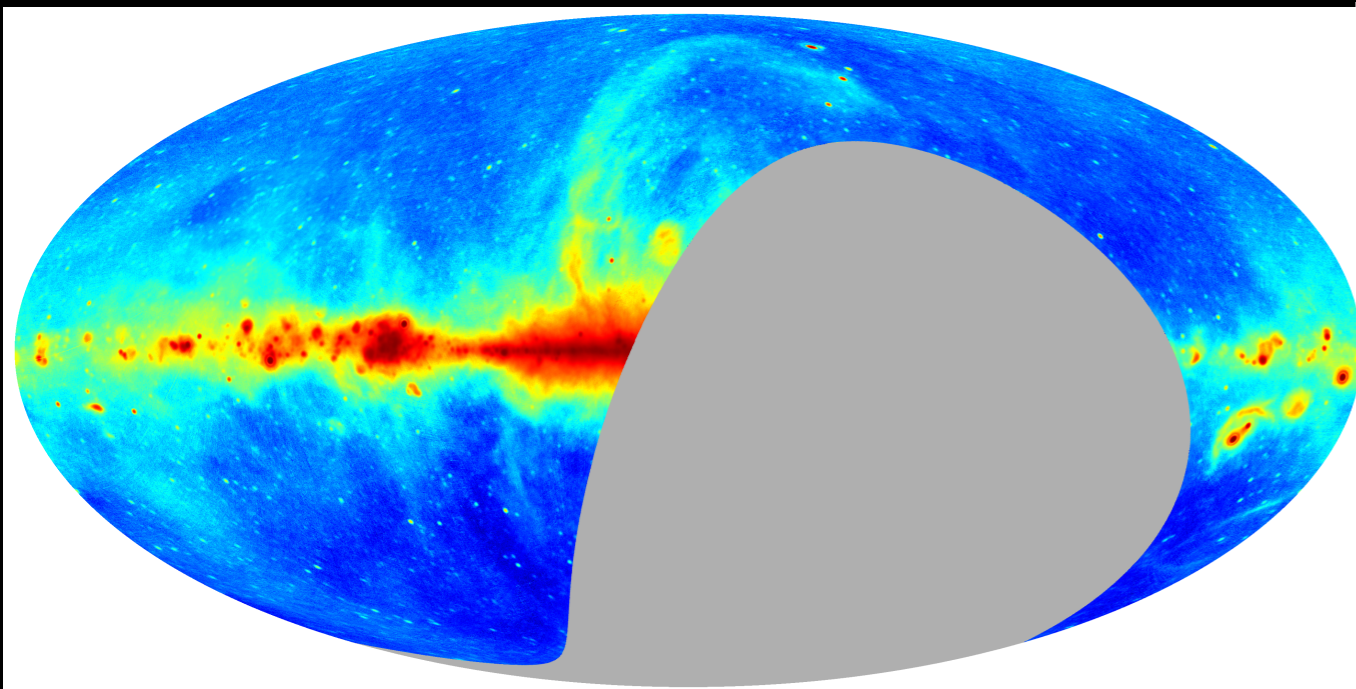


(139.1, 14.0)

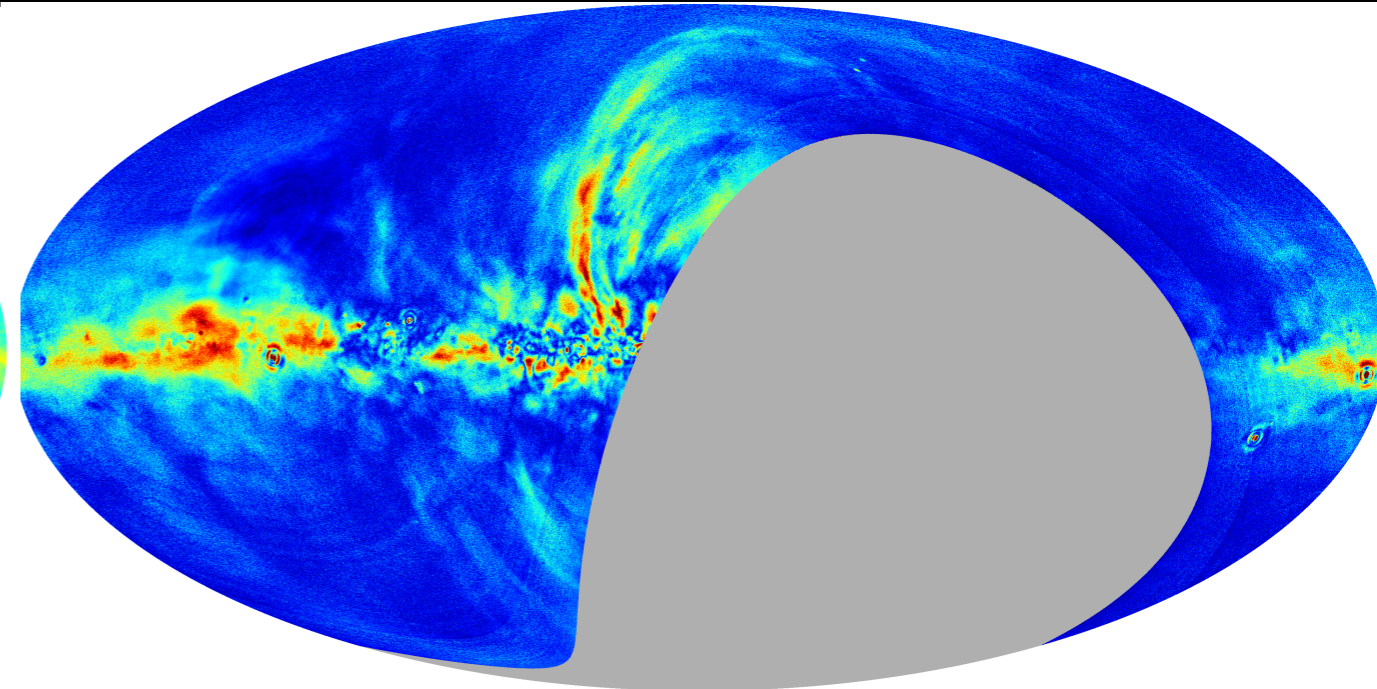


C-Band All-Sky Survey (C-BASS)

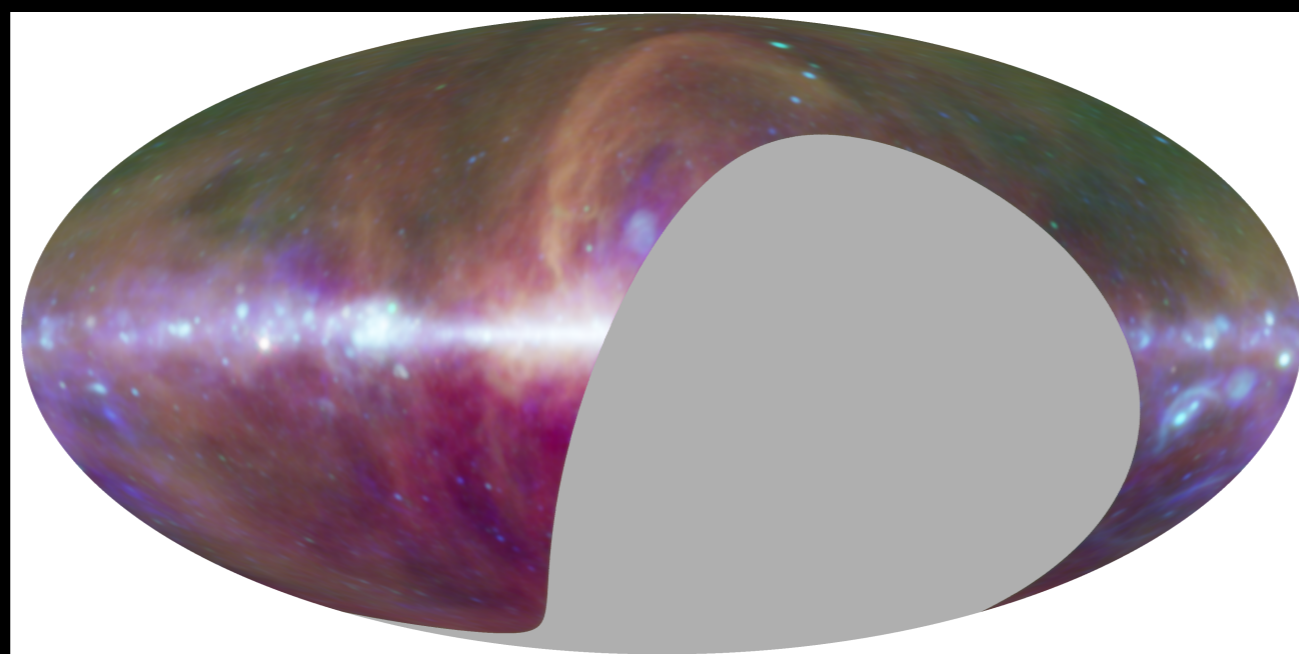
Definitive 5 GHz large-scale (~ 1 deg) survey
Watch out for results coming soon! (see Irfan et al. 2015)
Southern survey to begin soon!



Northern Intensity map



Northern Polarized intensity map



3-colour "spectral index" map

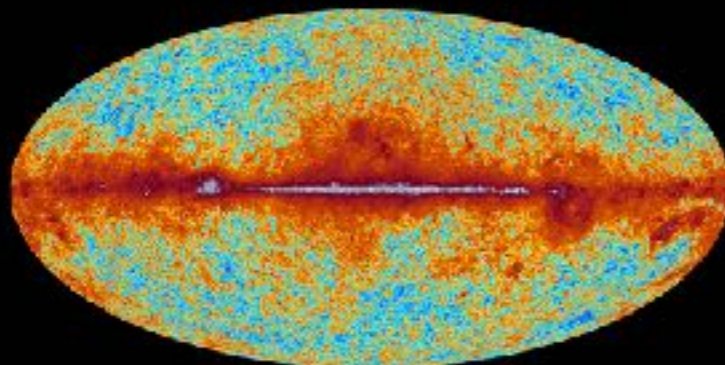
(Courtesy Luke Jew, U. Oxford)

High frequency maps (WMAP/Planck)

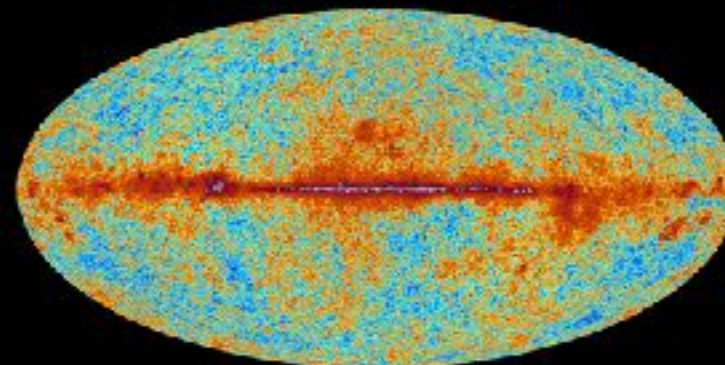


planck

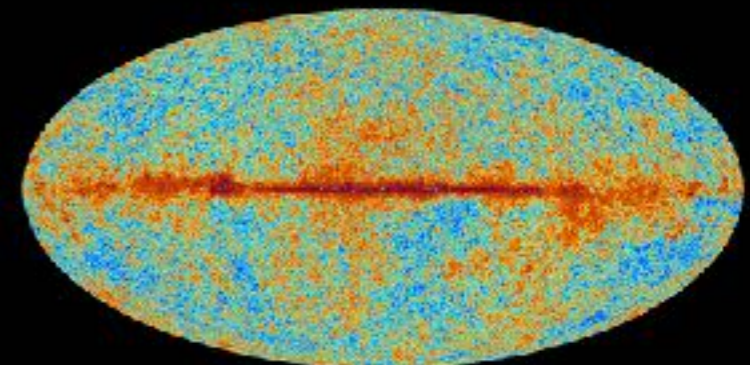
The sky as seen by Planck



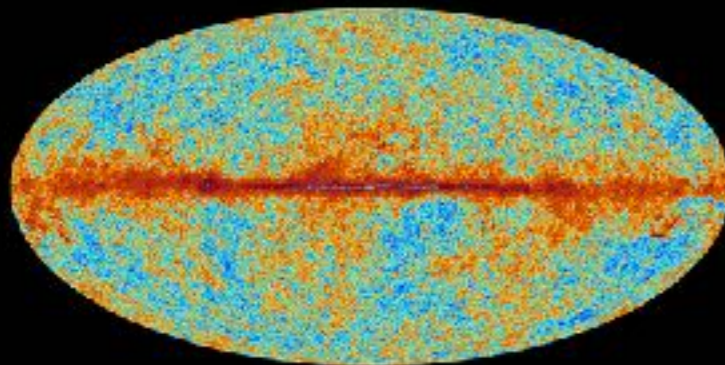
30 GHz



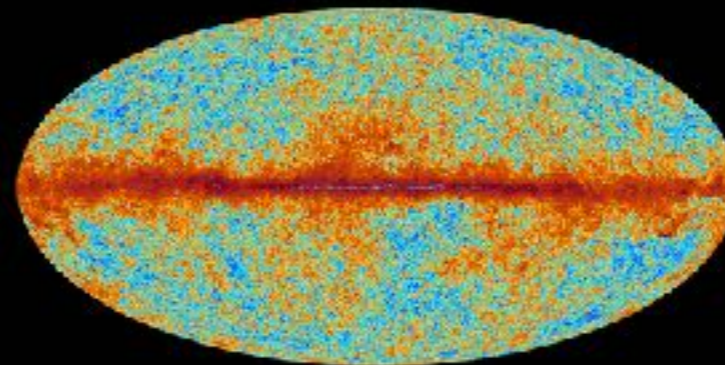
44 GHz



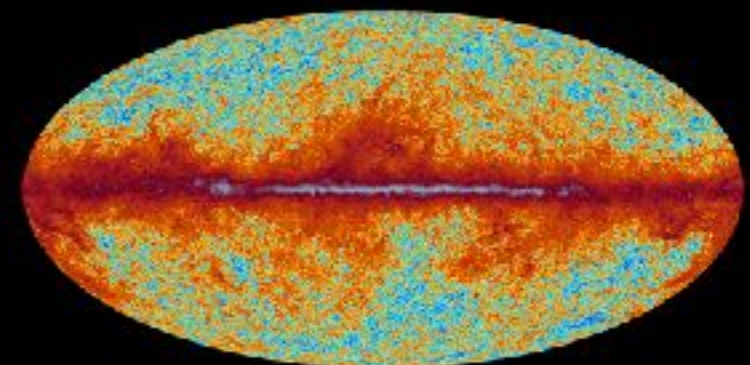
70 GHz



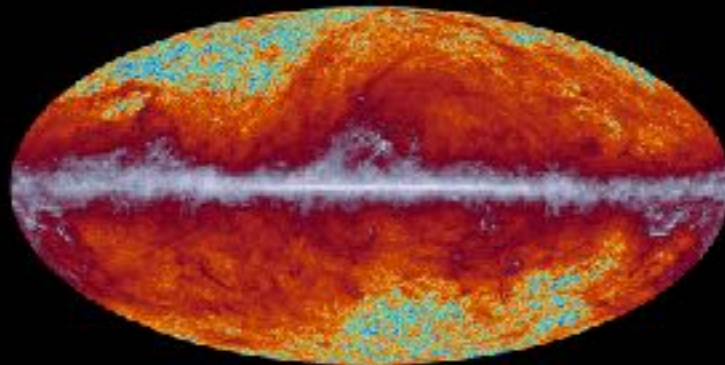
100 GHz



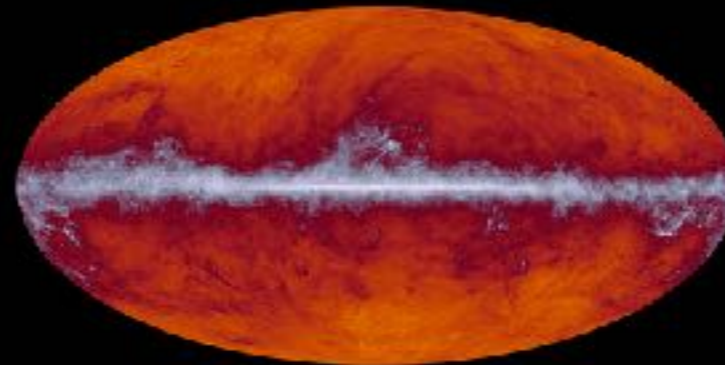
143 GHz



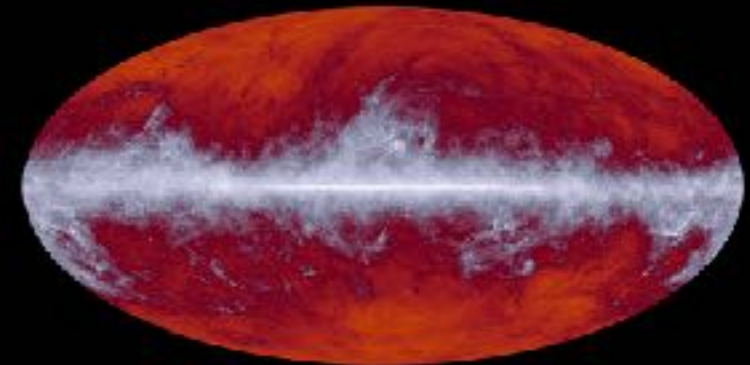
217 GHz



353 GHz



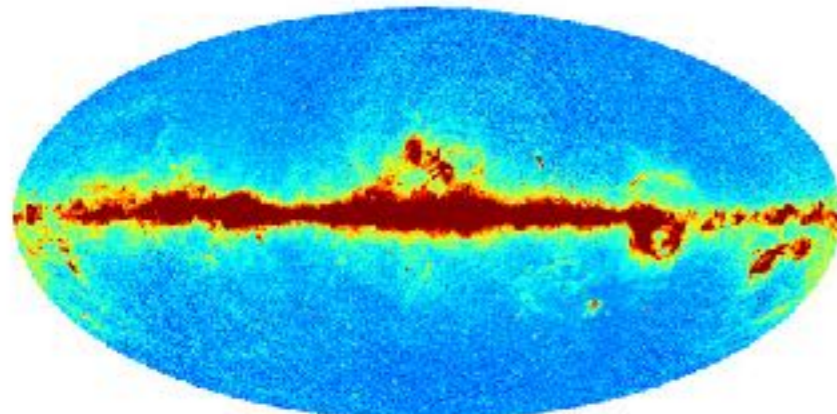
545 GHz



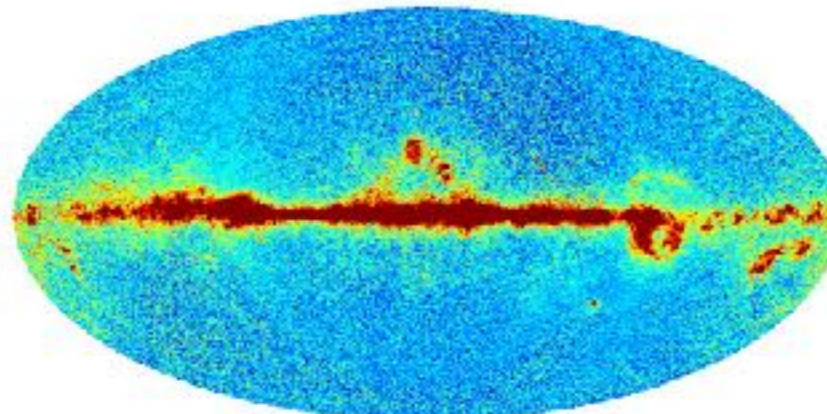
857 GHz

High frequency maps - CMB subtracted

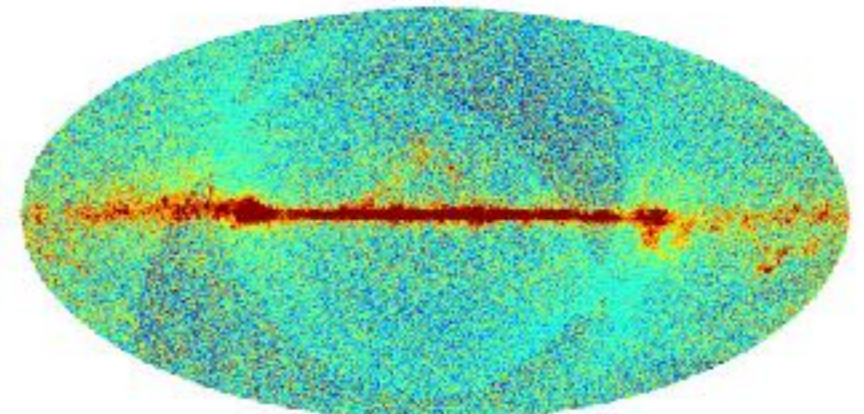
Planck all-sky foreground maps



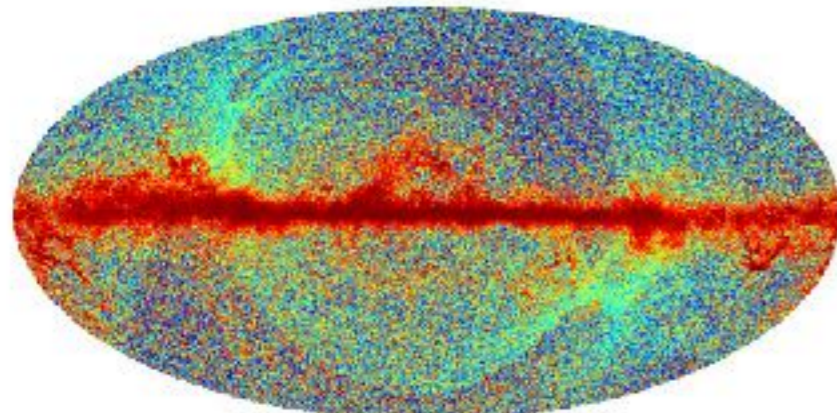
LFI 30 GHz



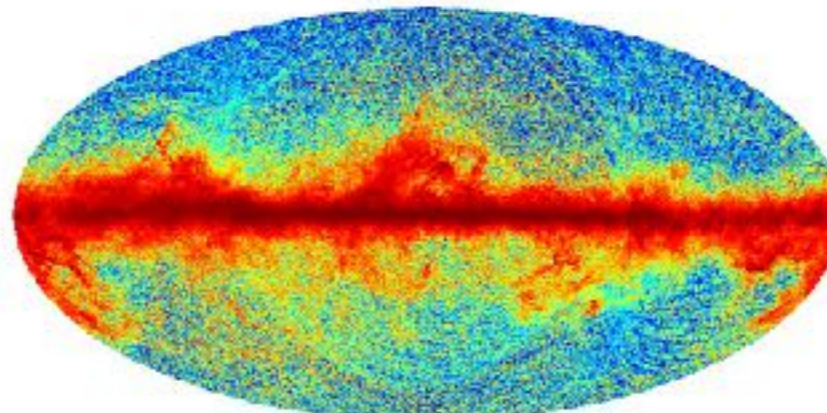
LFI 44 GHz



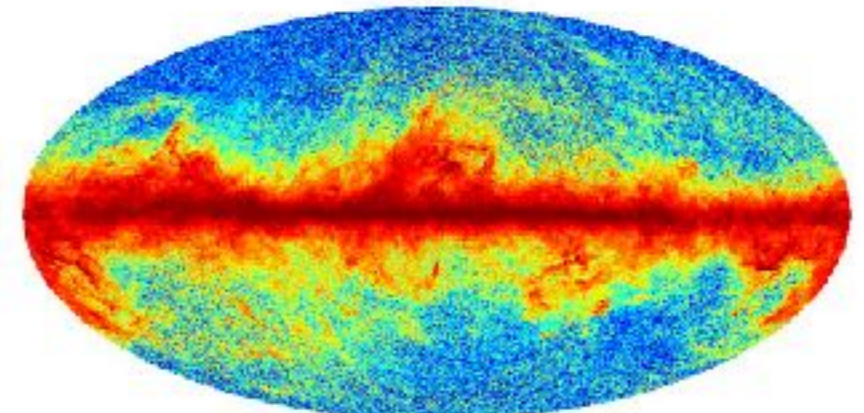
LFI 70 GHz



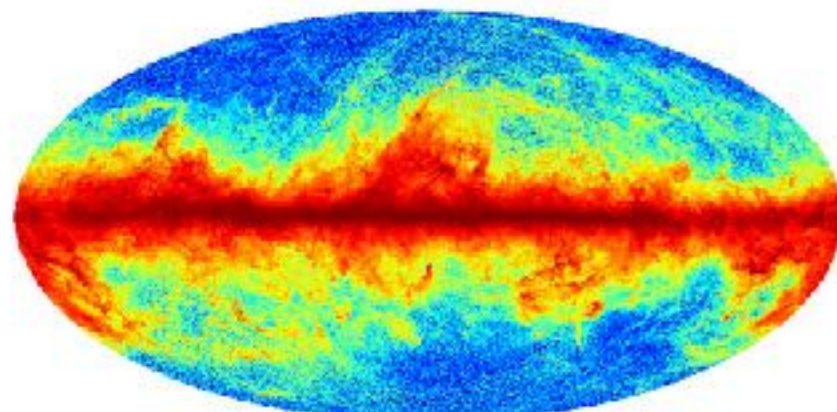
HFI 100 GHz



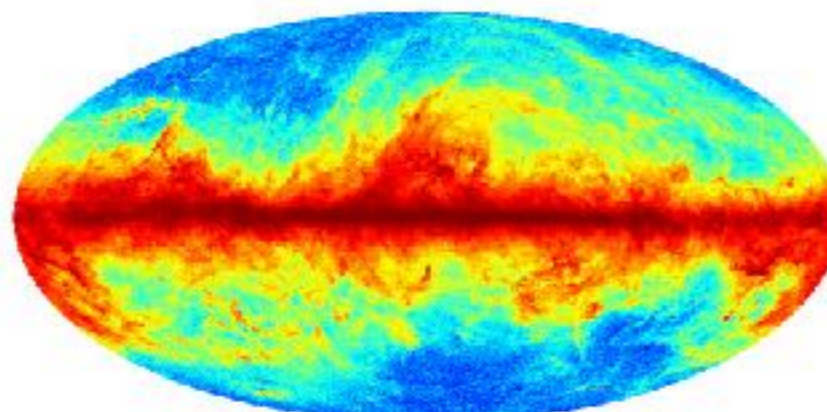
HFI 143 GHz



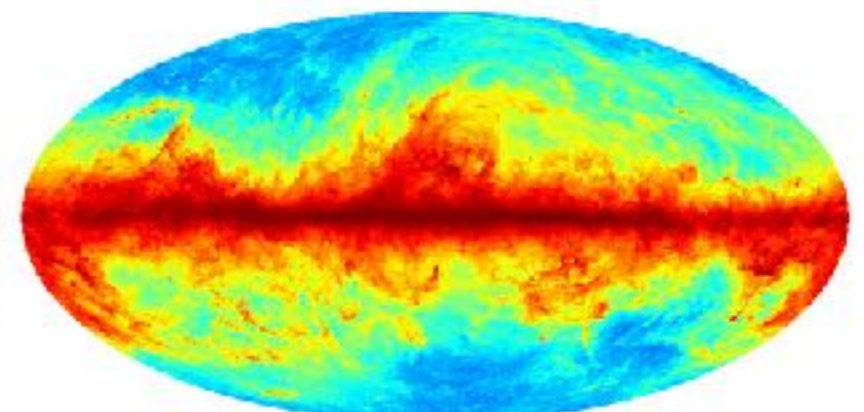
HFI 217 GHz



HFI 353 GHz



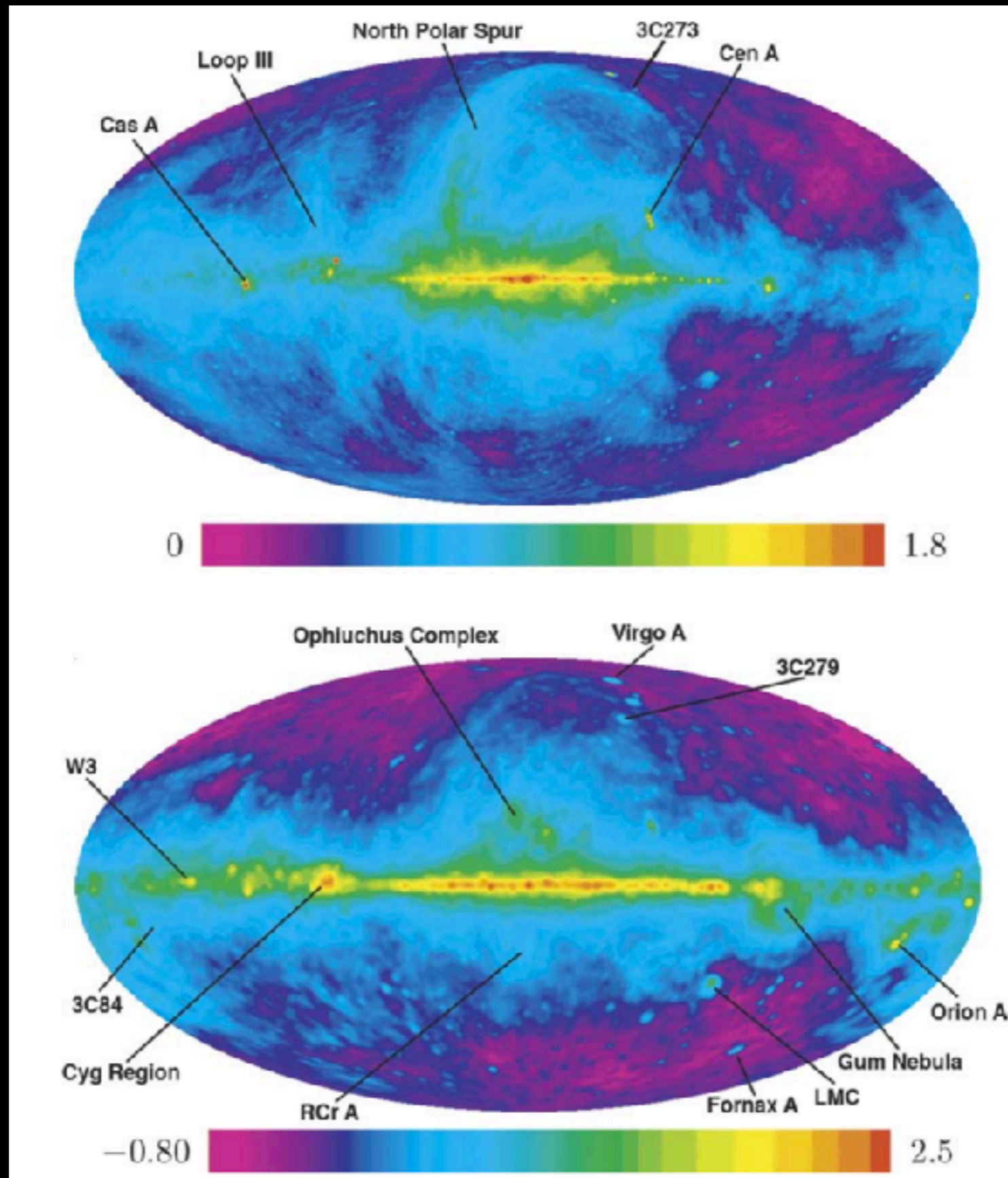
HFI 545 GHz



HFI 857 GHz

Intensity maps: low vs high frequency

Frequencies $> \sim 10$ GHz complicated mixture of several components



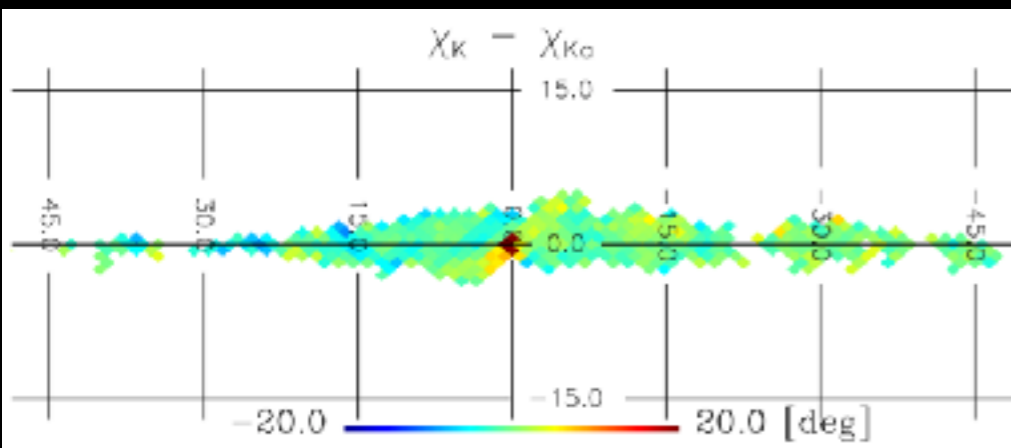
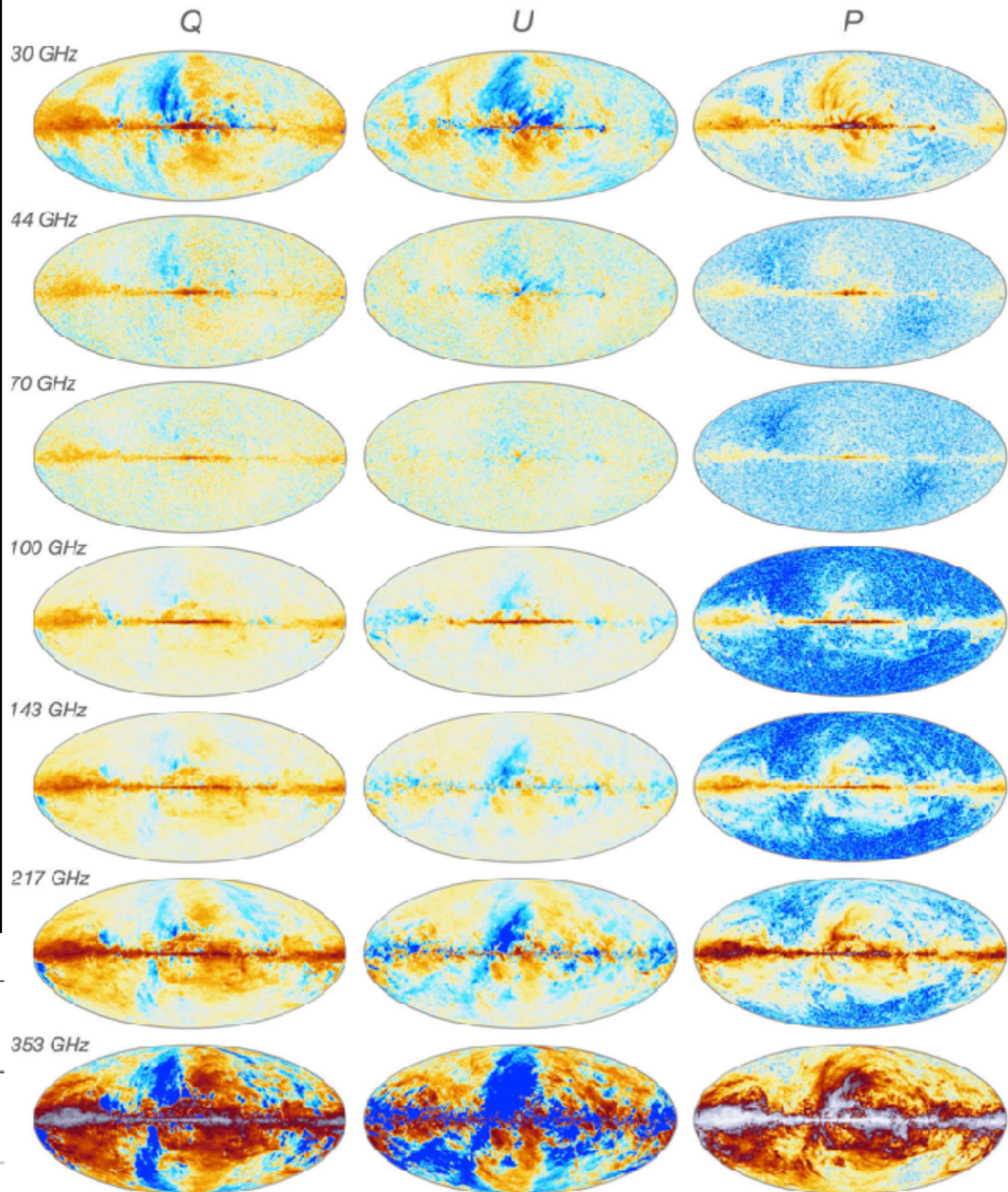
~ 1 GHz

~ 30 GHz

High frequency polarization maps from WMAP (23-94 GHz) and Planck (30-857 GHz)

Dominated by polarized synchrotron radiation in Faraday thin regime below 100 GHz and polarized thermal dust above 100 GHz

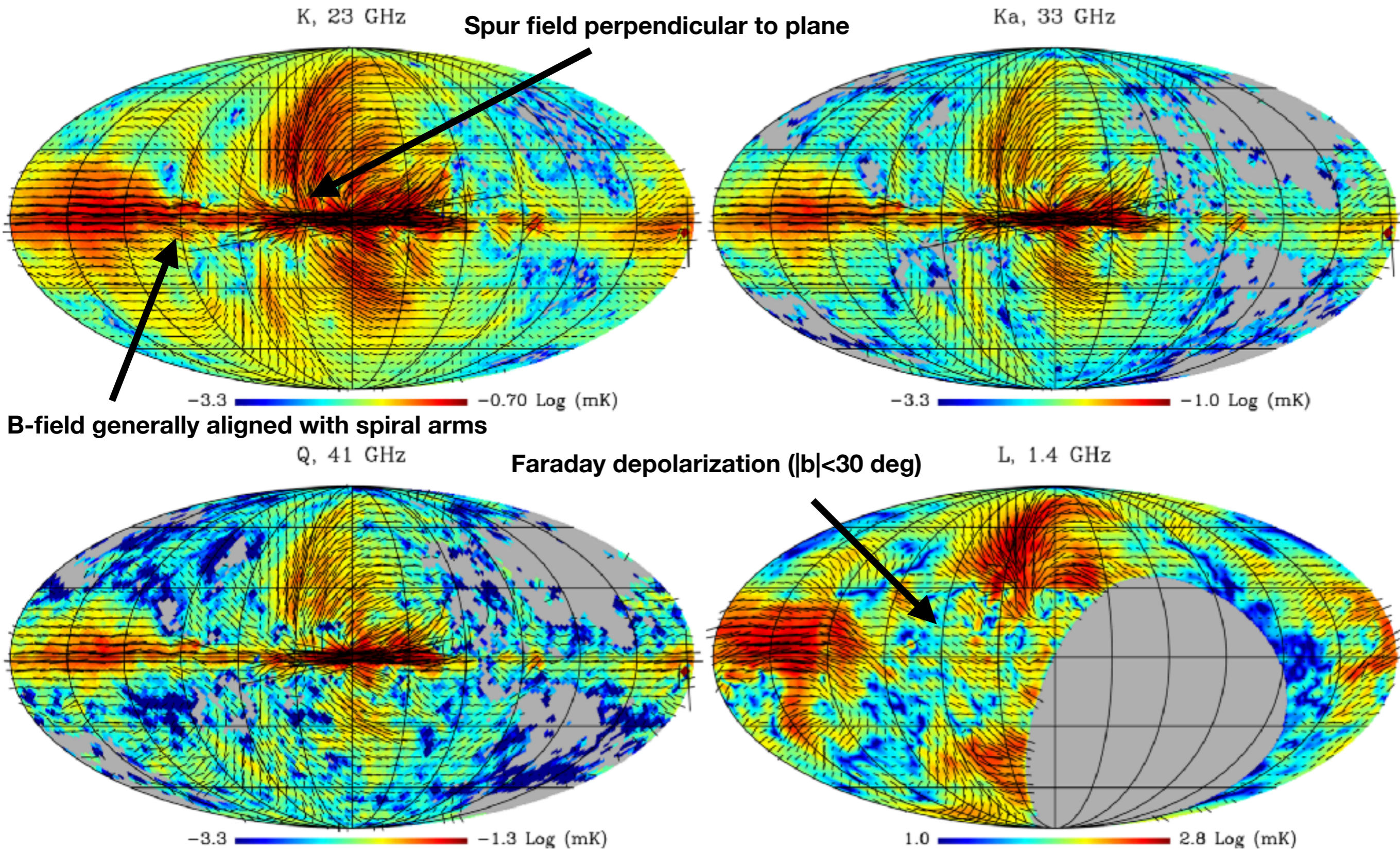
(No significant Faraday Rotation except near Galactic centre)



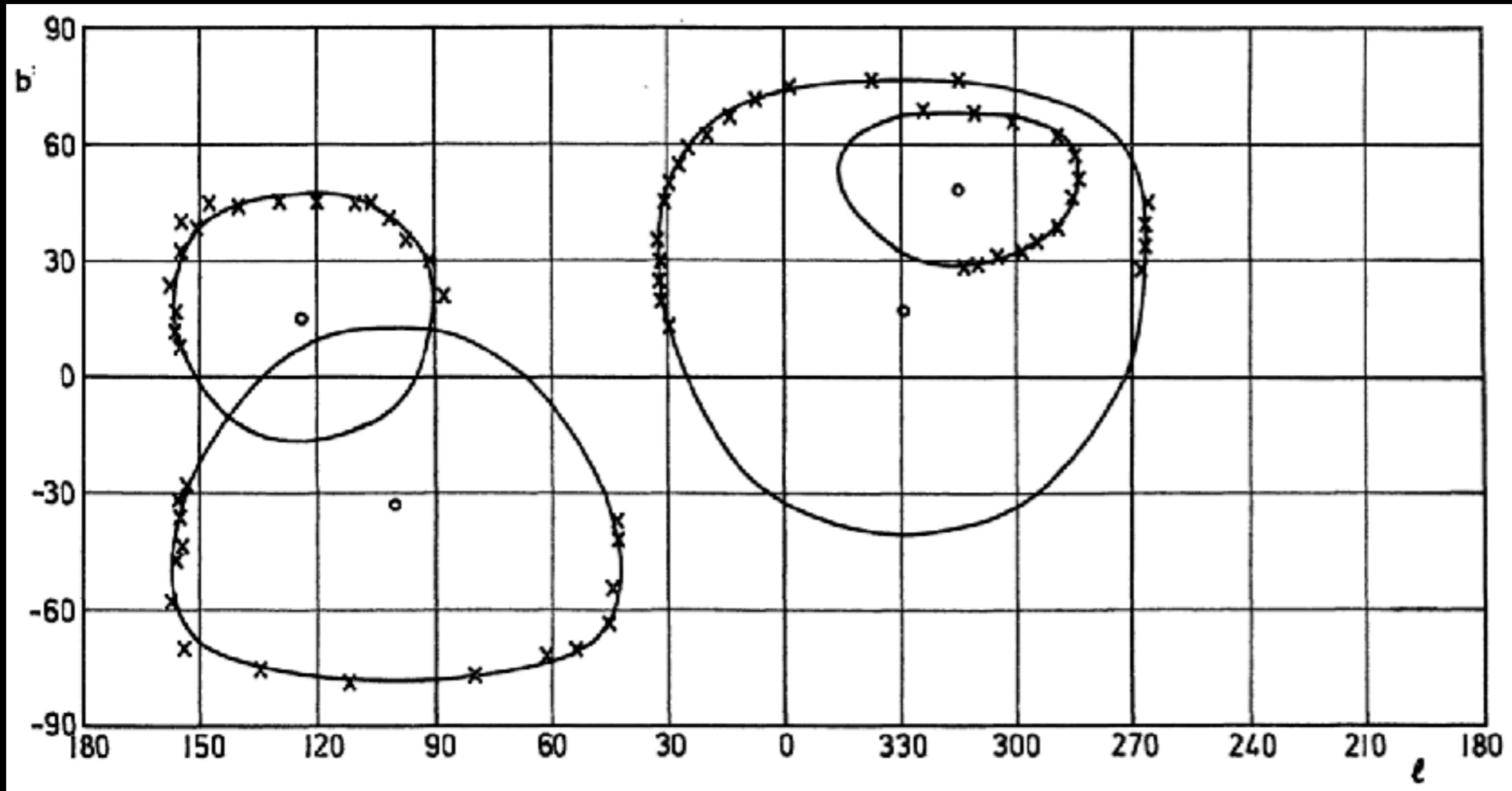
Projected magnetic field direction above a few GHz

(rotate synchrotron angle by 90 deg)

Vidal et al. (2015)



4 main radio loops



Object	l (centre)	b (centre)	Diameter	R. M. S. Deviation	Arc Length
Loop I	$329^\circ \pm 1.5$	$+17.5 \pm 3^\circ$	$116^\circ \pm 4^\circ$	0.9	155°
Loop II	$100^\circ \pm 2^\circ$	$-32.5 \pm 3^\circ$	$91^\circ \pm 4^\circ$	1.1	150°
Loop III	$124^\circ \pm 2^\circ$	$+15.5 \pm 3^\circ$	$65^\circ \pm 3^\circ$	1.7	180°
Loop IV	$315^\circ \pm 3^\circ$	$+48.5 \pm 1^\circ$	$39.5 \pm 2^\circ$	0.8	190°

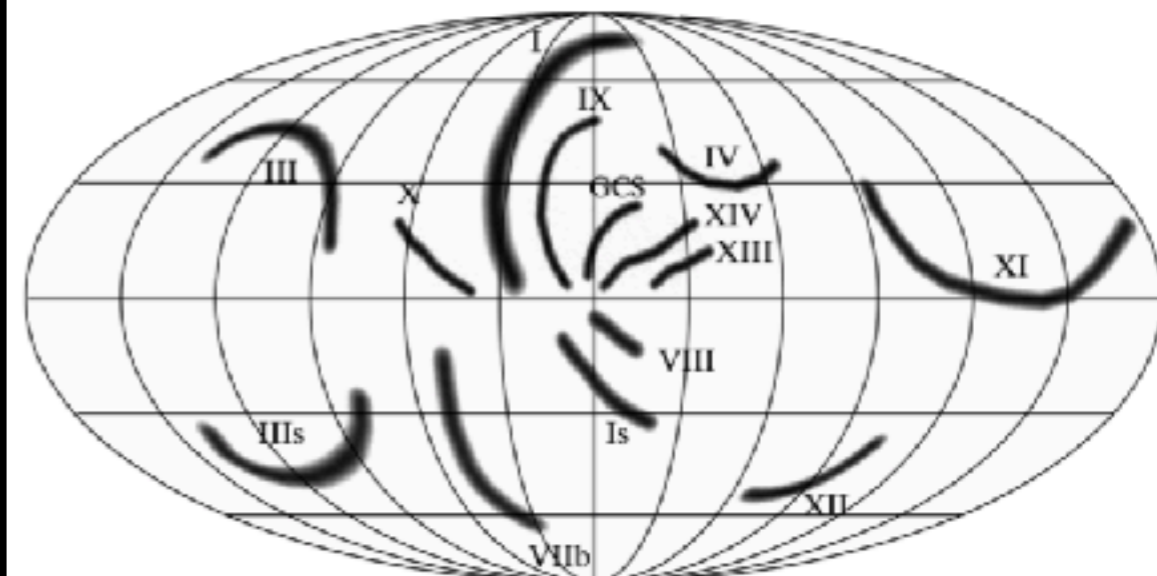
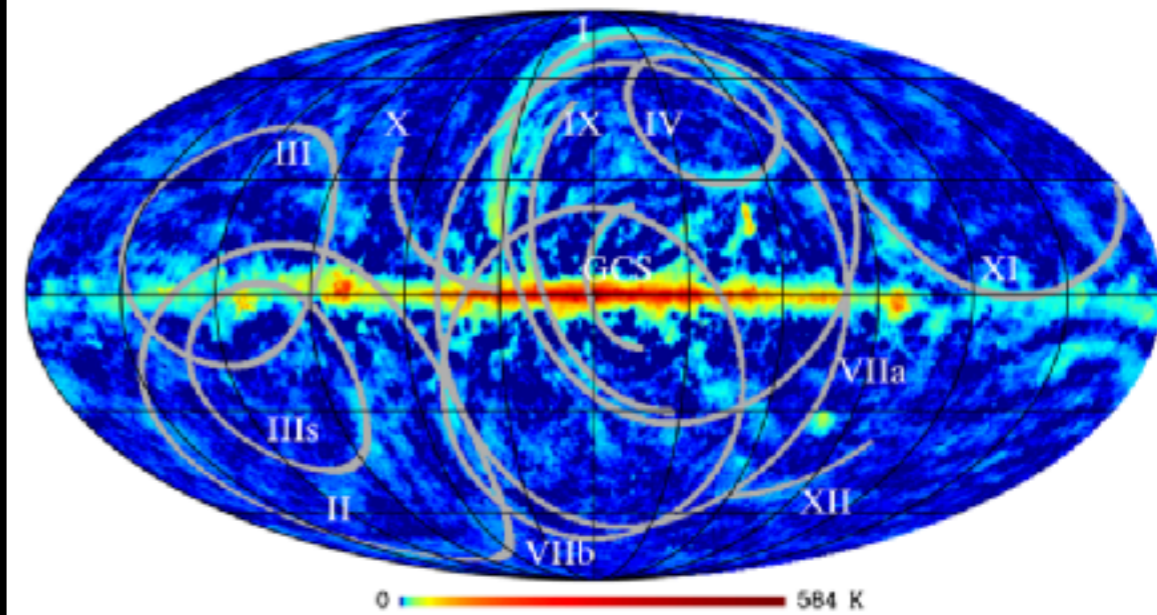
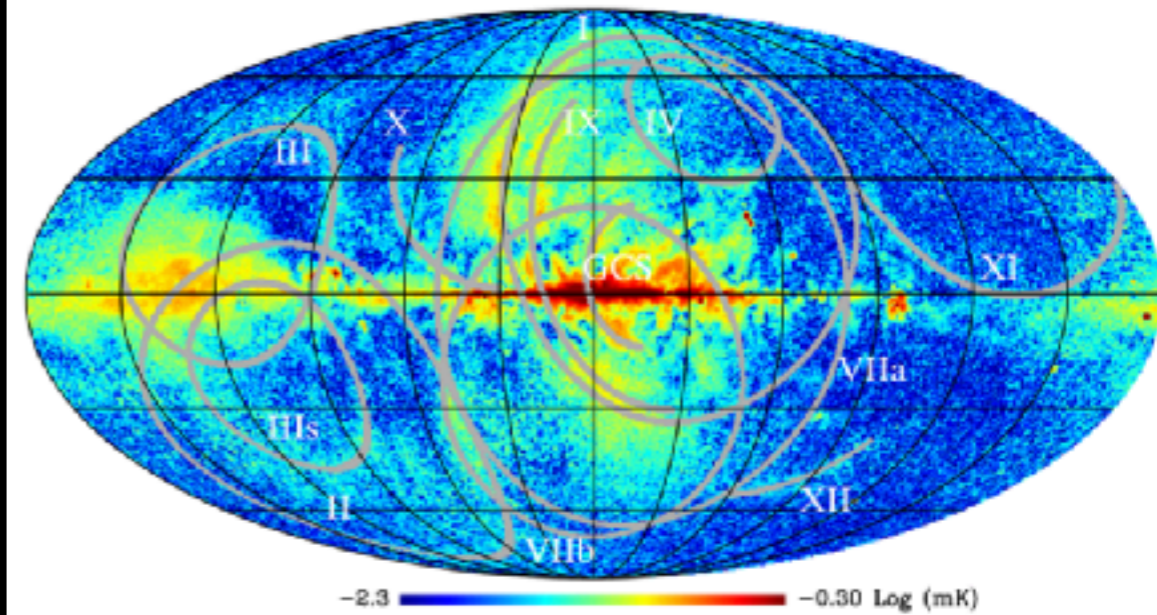
A new look at polarized spurs and filaments

Vidal, Dickinson, Leahy (2015)

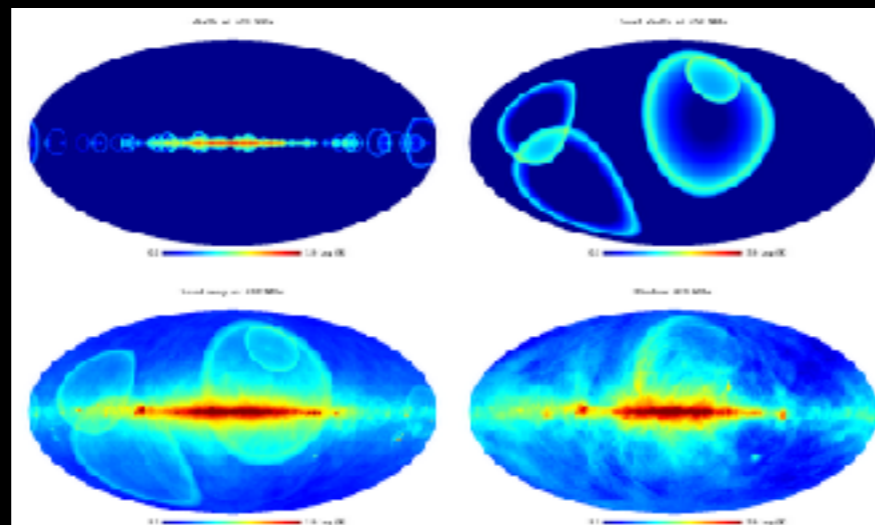
Identified several new filaments/spurs
Some only seen in polarization

Loop name	Continuum			Polarization			Comments / reference
	<i>l</i>	<i>b</i>	<i>r</i>	<i>l</i>	<i>b</i>	<i>r</i>	
I	329.0	17.5	58	332.6	20.7	54.3	NPS, Brown et al. (1960)
II	100.0	-32.5	45.5	-	-	-	Large et al. (1962)
III	124.0	15.5	32.5	118.8	13.2	31.6	Quigley & Haslam (1965)
IV	315.0	48.5	19.8	315.8	48.1	19.3	Large et al. (1966)
V	127.5	18.0	67.2	-	-	-	Milogradov-Turin & Urošević (1997), same as VI
VI	120.5	30.8	72.4	-	-	-	Milogradov-Turin & Urošević (1997), not same as V
GCS	-	-	-	344.0	4.8	18.5	Galactic Centre Spur from Sofue, Reich & Yamamoto (2001)
III _s ^a	-	-	-	106	-22	50.0	Below the plane at the 'fan' region.
VIIa	-	-	-	345.0	0.0	65	From Wolleben (2007) using the 1.4 GHz continuum emission
VIIb ^a	-	-	-	0.7	-23.3	45.9	Values found in this work for VIIa.
IX ^a	-	-	-	332.0	16	46.5	Inside the NPS.
X ^a	-	-	-	30	35	67.0	Tangential to the plane.
XI ^a	-	-	-	227	38	81.0	Large arc tangential to the plane.
XII	-	-	-	300	0.7	27.6	Close to the LMC.
VIII	-	-	-	-	-	-	Southern part of the GCS?
XIII	-	-	-	-	-	-	Weak continuum emission at 0.408 GHz.
XIV	-	-	-	-	-	-	Possible H I counterpart (see Section 7.1).

Note. ^aThese arcs are clearly visible only in polarization.

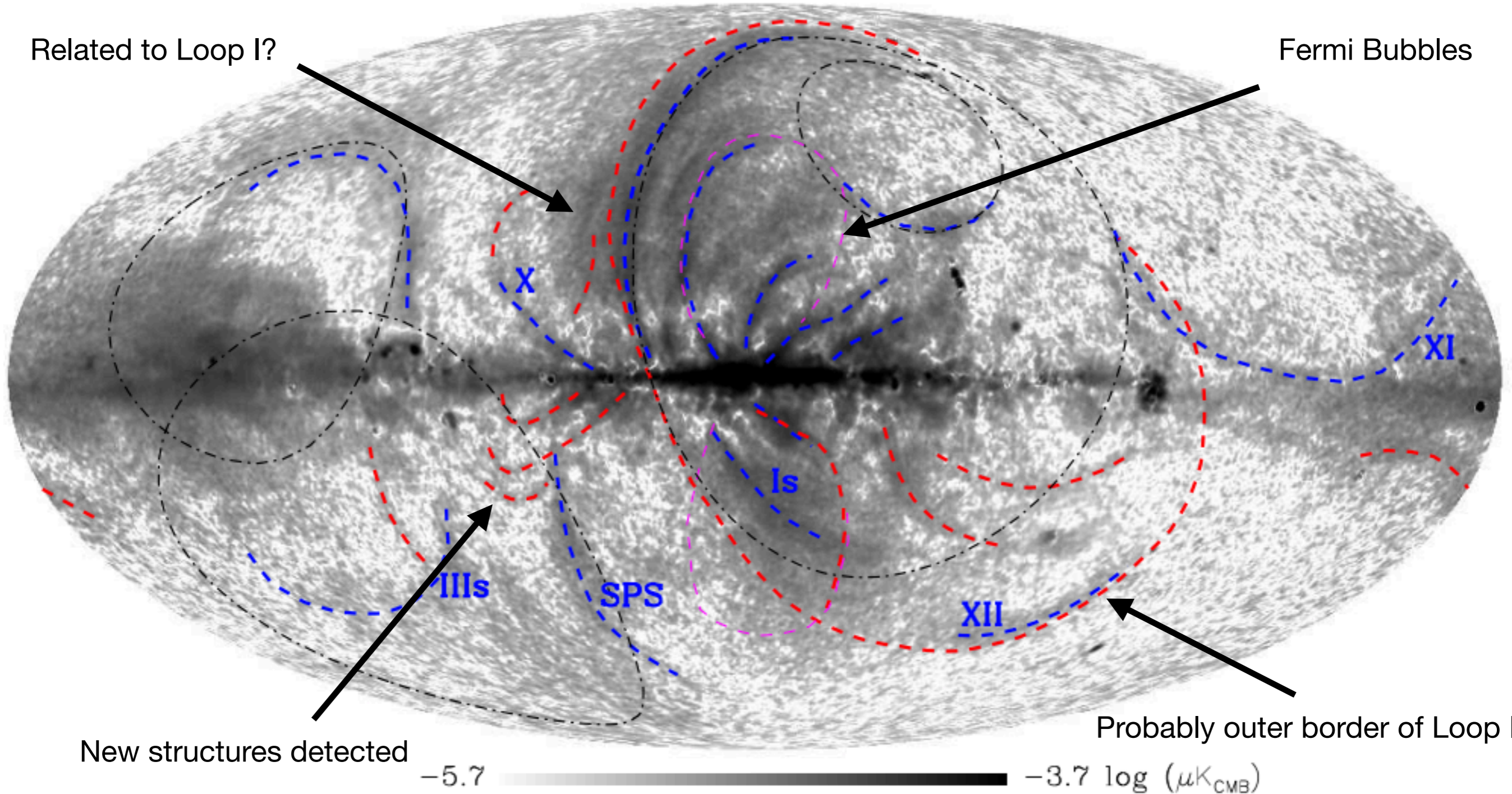


Mertsch & Sarkar (2013) model quite compelling since we would only clearly see nearby/high latitude structures



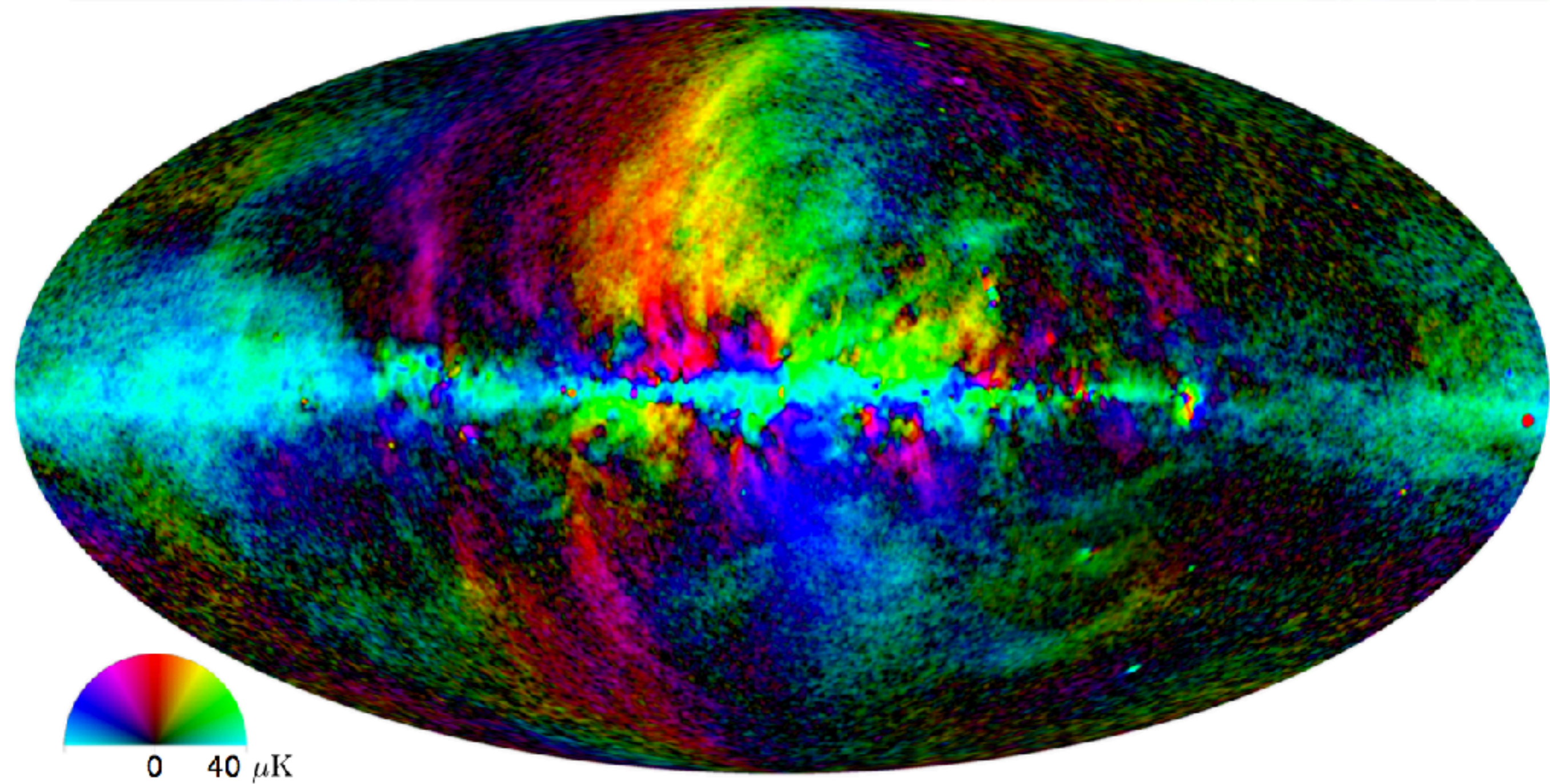
High S/N synchrotron polarized intensity map

Combined WMAP+Planck map at 23 GHz in Faraday-thin region
Optimal noise weighting, remove missing WMAP modes etc.



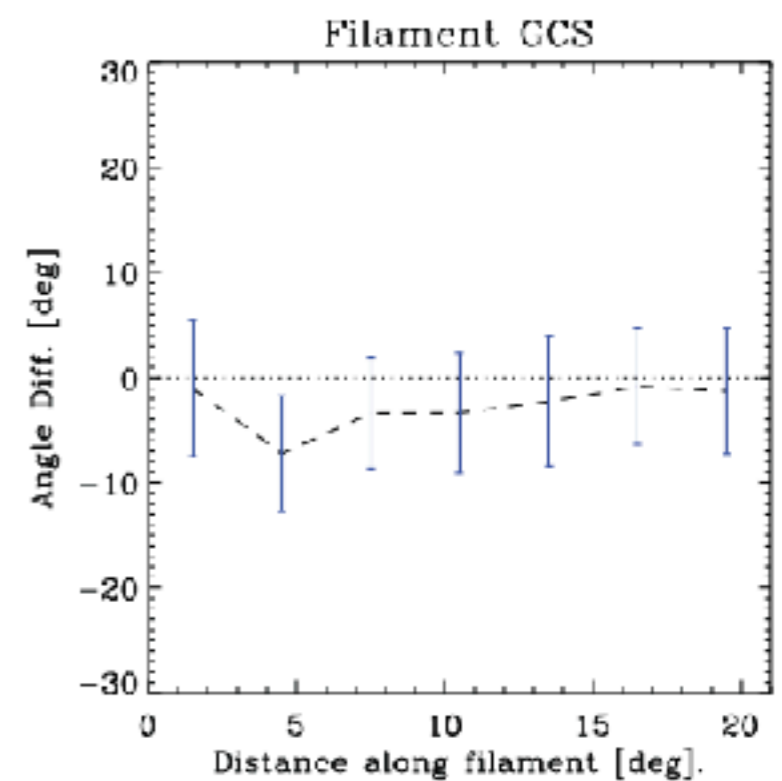
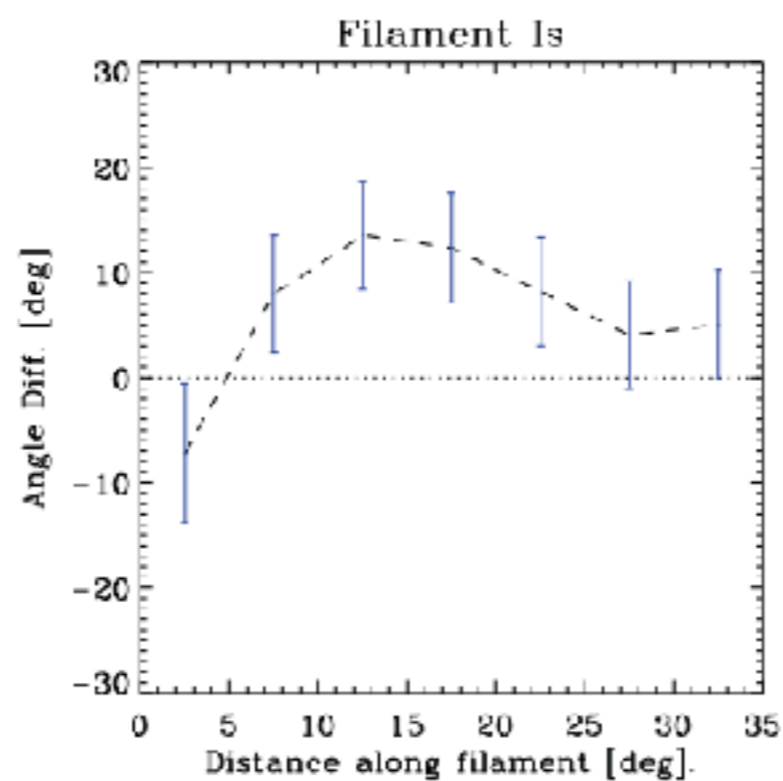
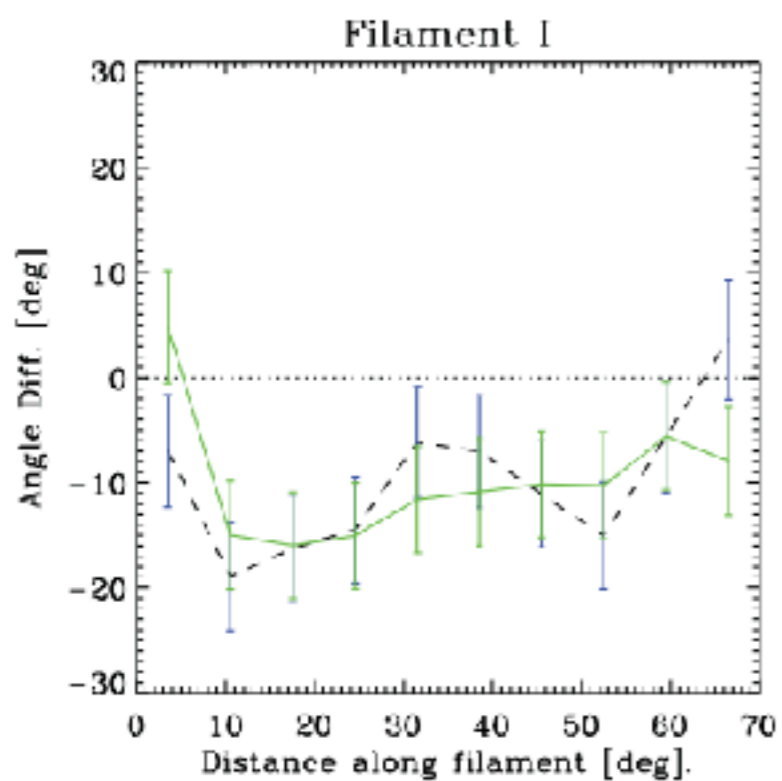
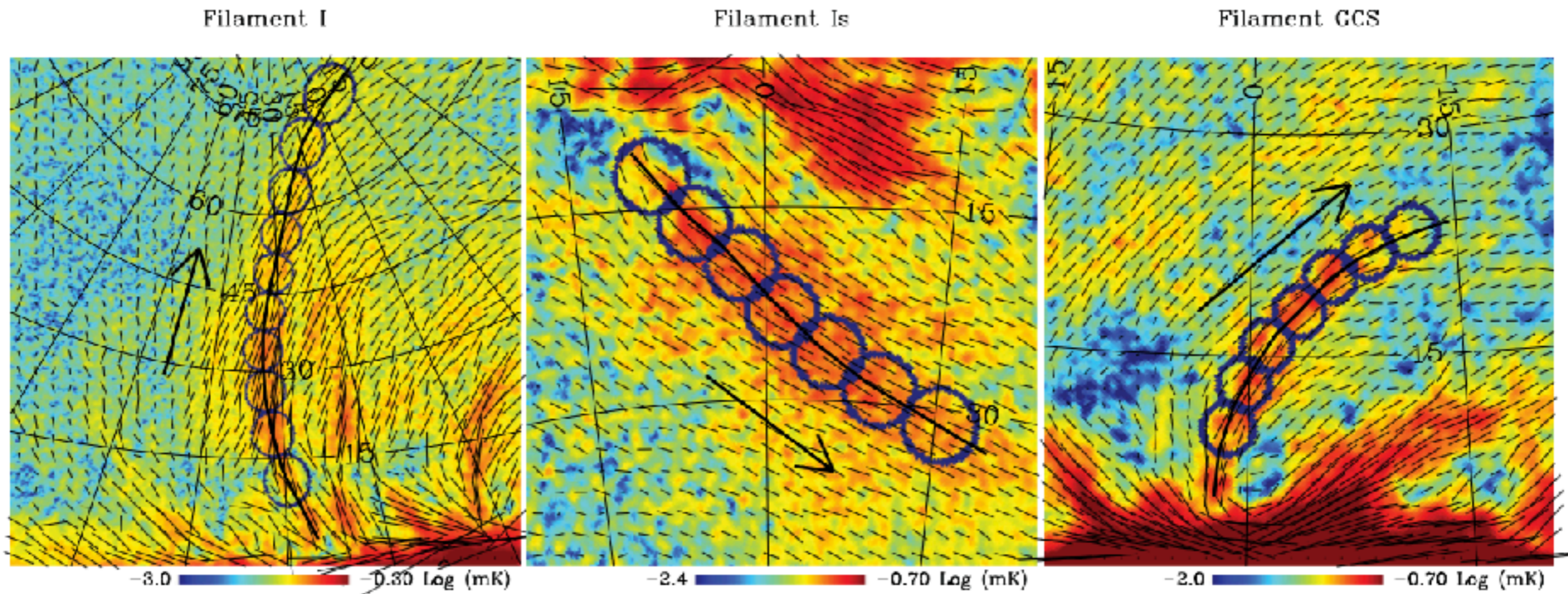
High S/N synchrotron polarized intensity map

Lots of (overlapping) coherent large-scale structures!



Magnetic field approx follow ridges of loops/spurs (but not always/exactly!)

Vidal et al. (2015)

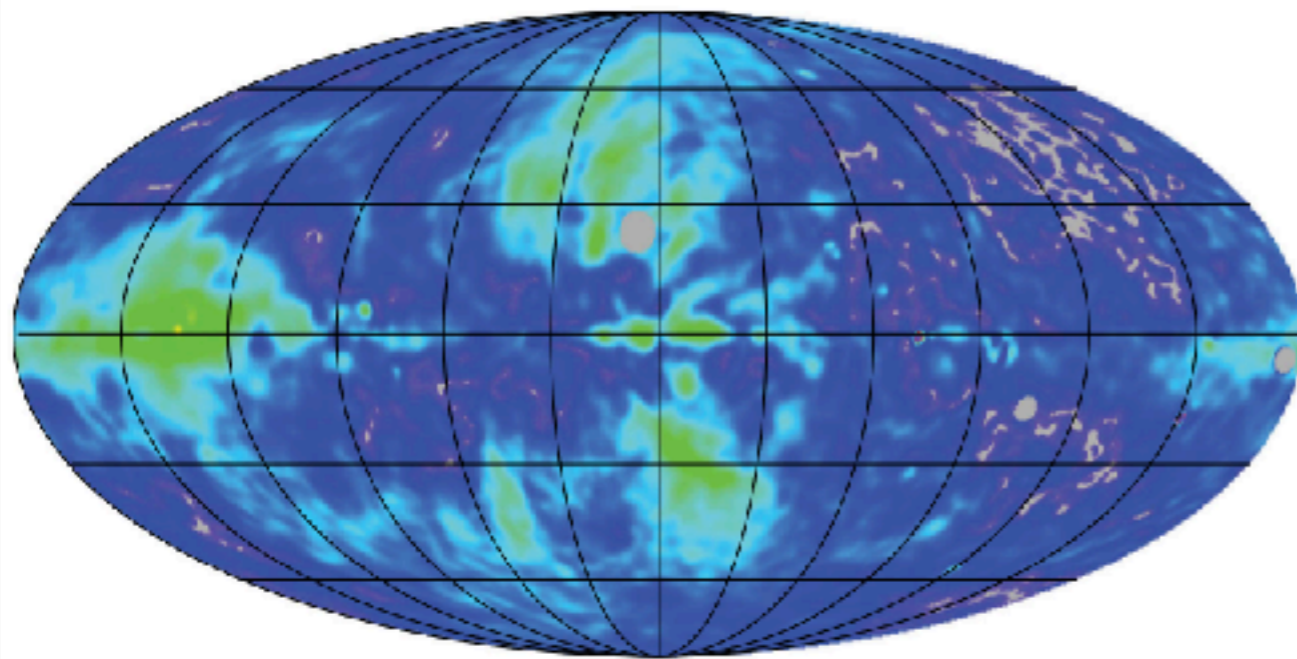


Synchrotron polarization fraction

Vidal et al. (2015)

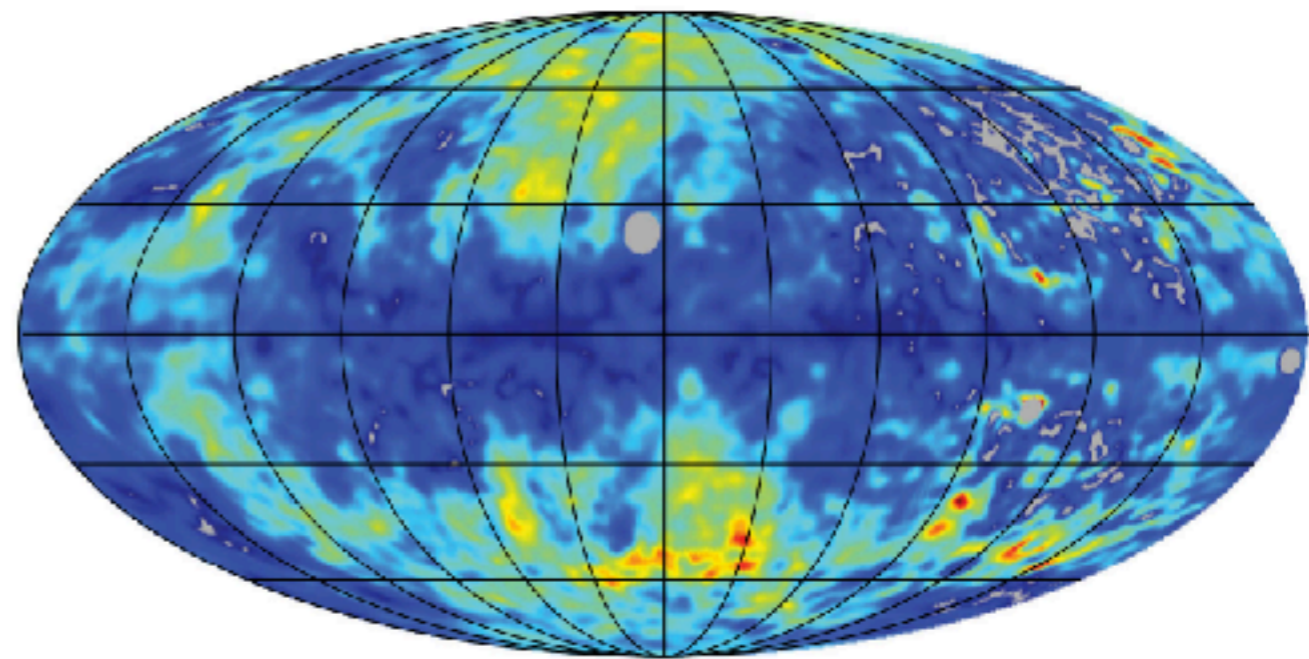
Zero levels and component separation in intensity difficult to be accurate

Synch. Pol. Fraction, $\beta = -3.0$



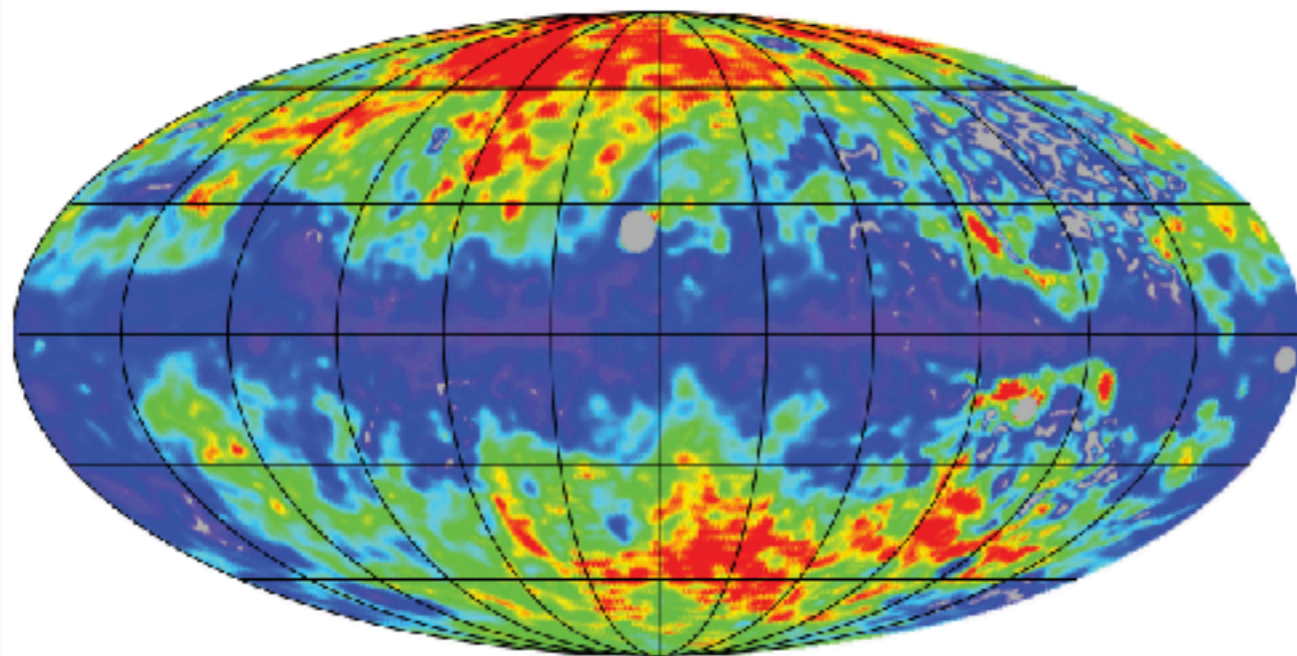
0.0 70.0 %

Synch. Pol. Fraction, using MEM



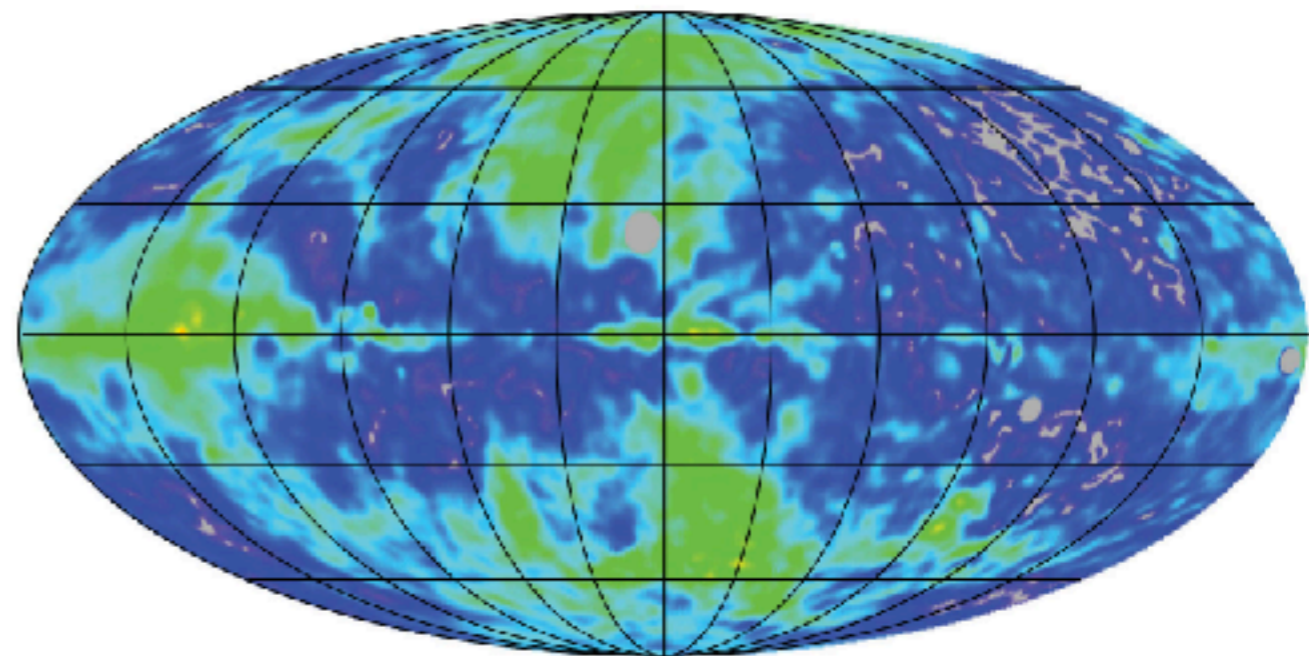
0.0 70.0 %

Synch. Pol. Fraction, using MCMC model c



0.0 70.0 %

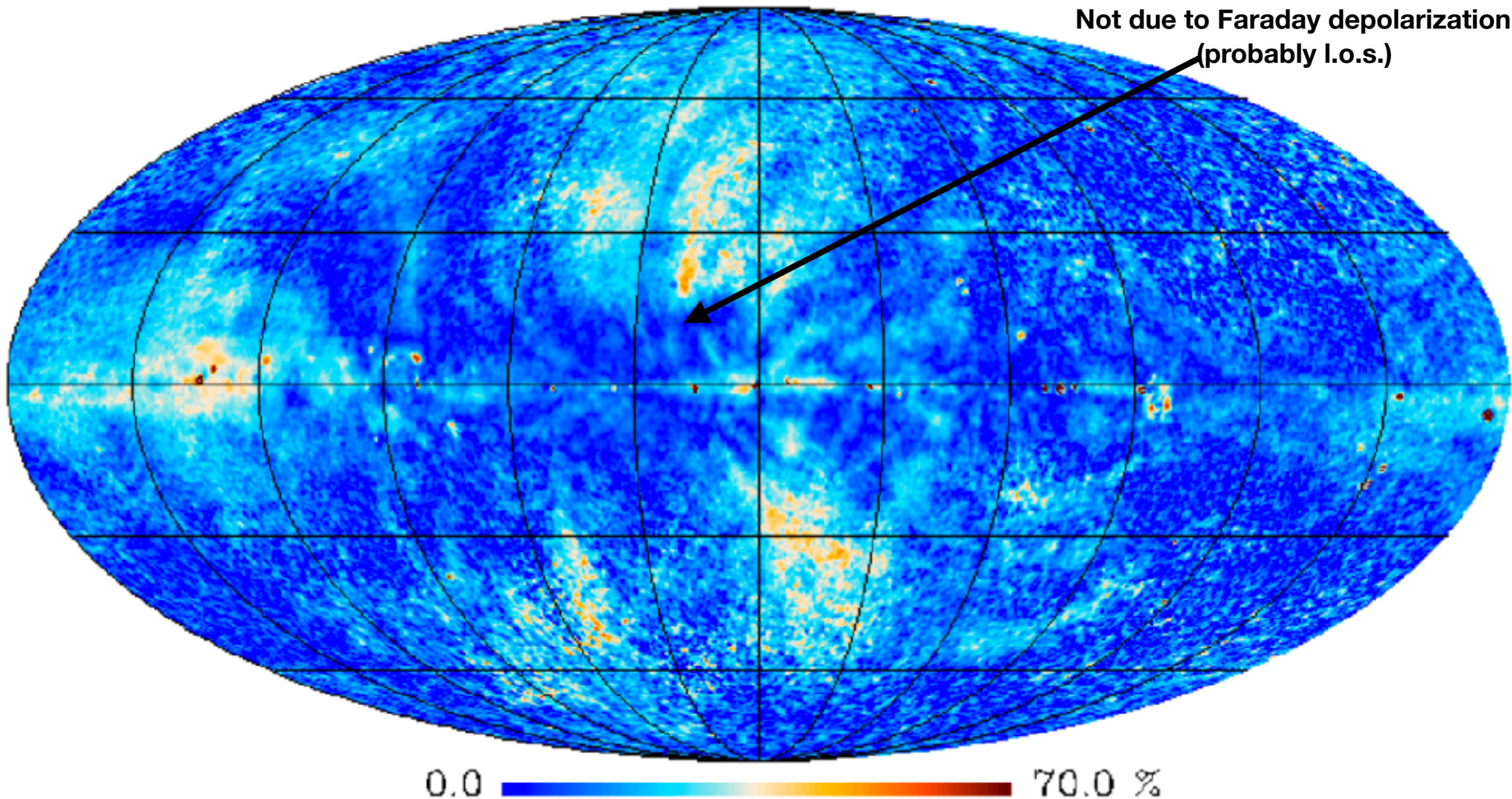
Synch. Pol. Fraction, using MCMC model e



0.0 70.0 %

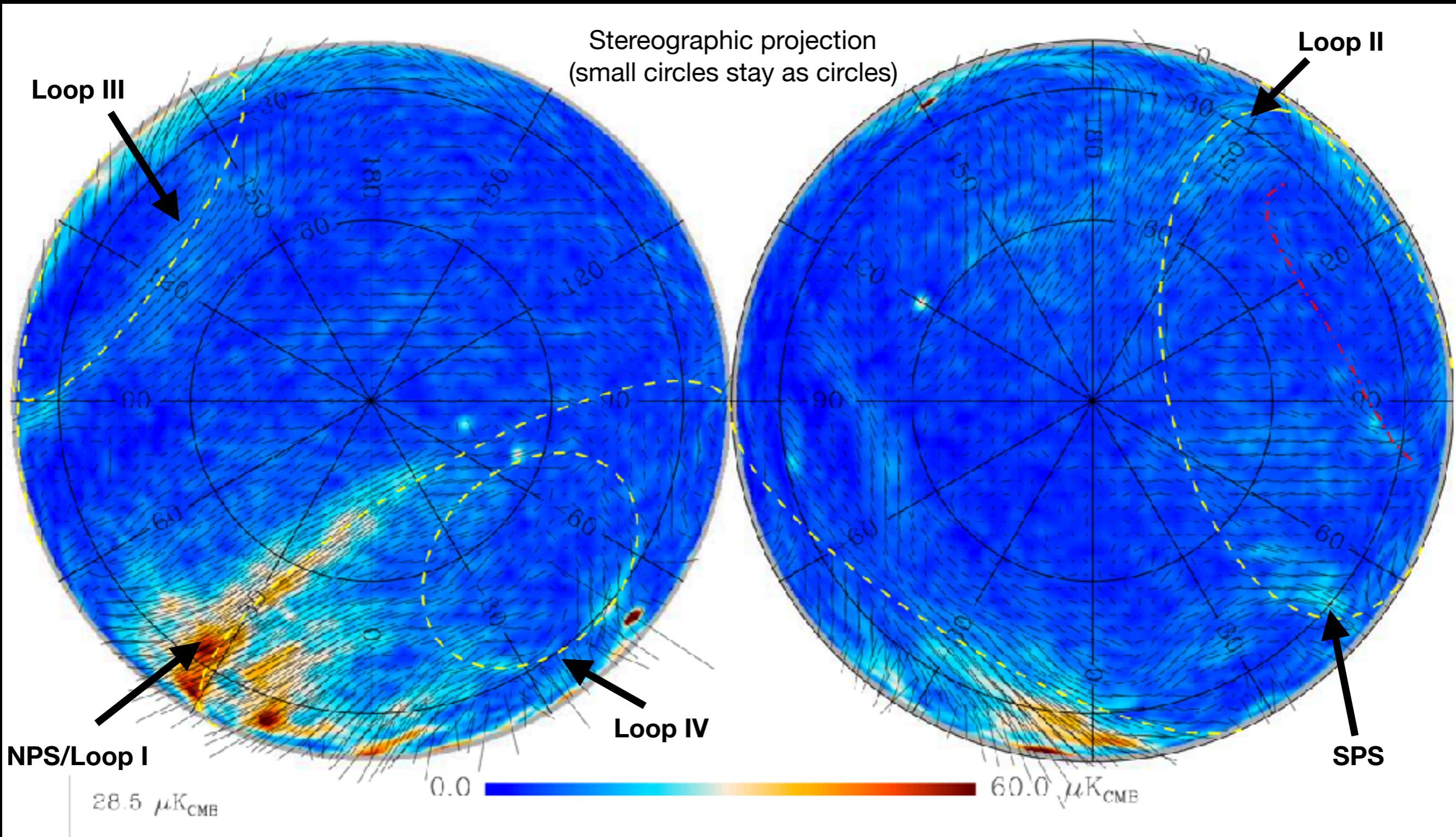
Synchrotron polarization fraction

Polarization fractions up to ~40-50% suggest very coherent magnetic field
(theoretical max~75% therefore very little depolarization)



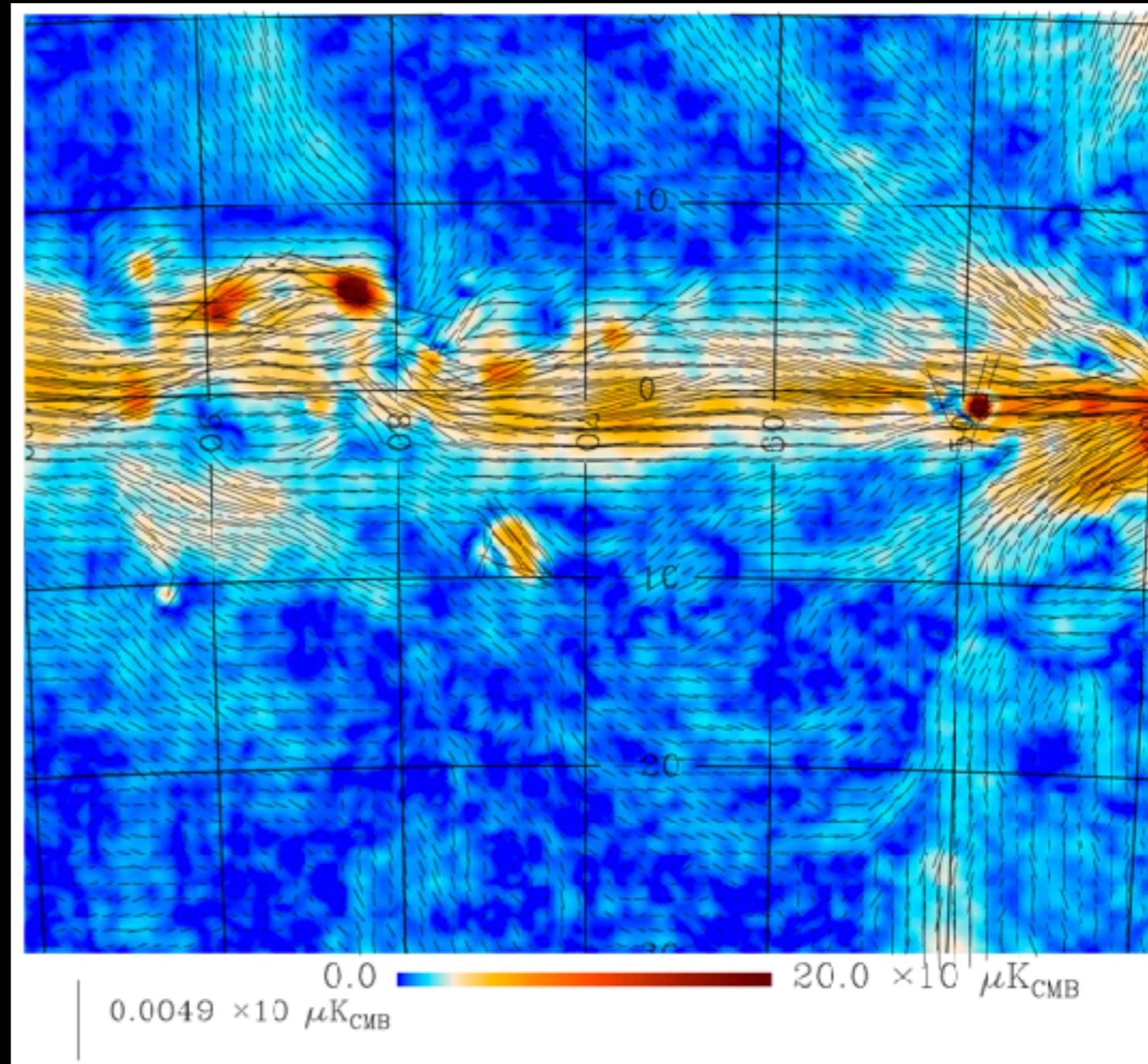
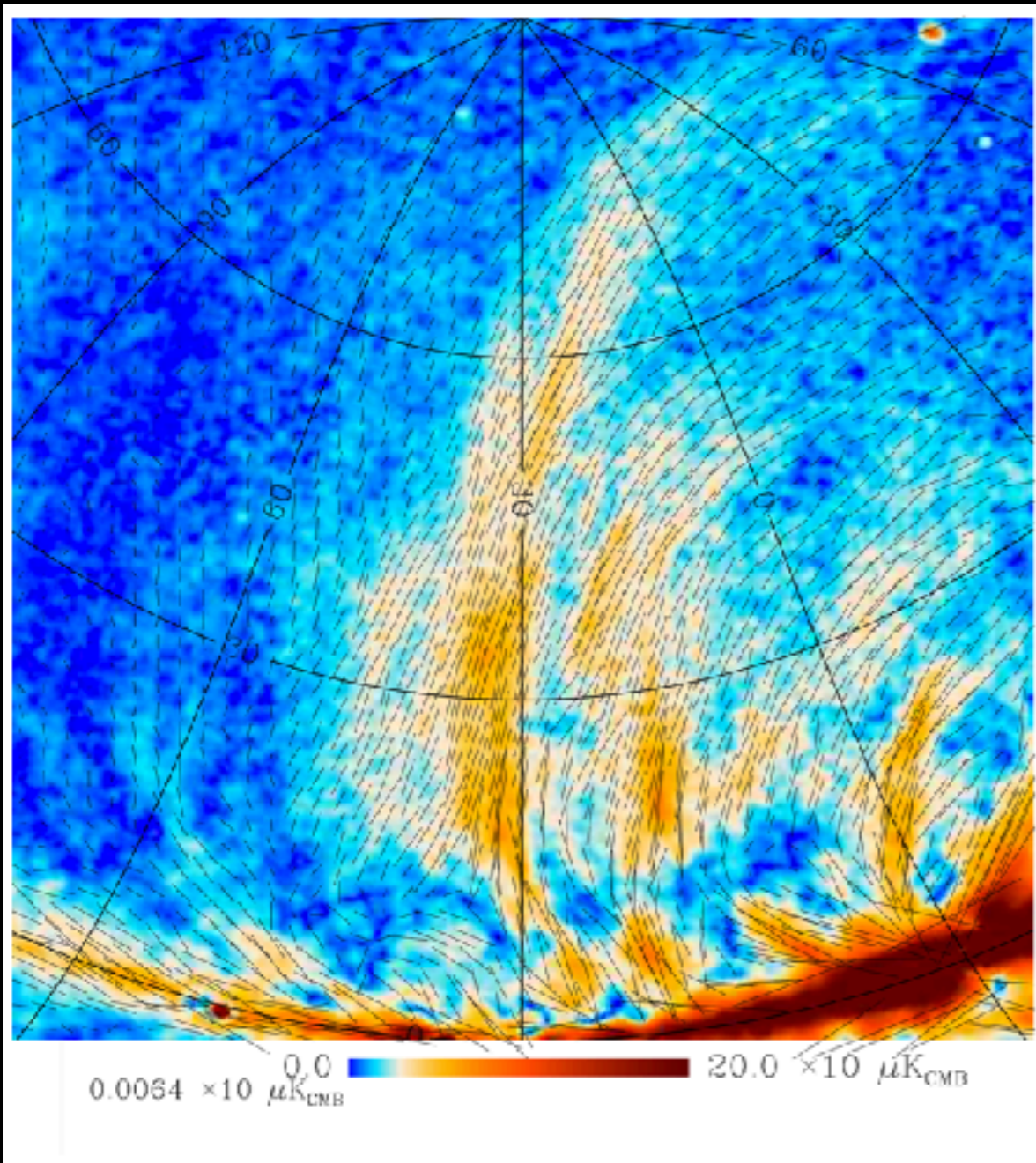
Loops in polarization

- B-field aligned with NPS/Loop I well outside loop boundary
- South Polar Spur (SPS) not related to Loop II (Cetus arc) as originally thought nor Loop I
 - But does have its own cold HI/dust outer border (another loop?)



More filaments, spurs, loops, arcs!

- Several internal spurs with similar orientation (multiple shocks/SNe?)
- Outer emission beyond NPS could be different structures?
- Additional filaments e.g. filament X which curves over strongly (looks like Fermi Bubble!), l=45 filament, Orion-Taurus filament etc...
- Several more visible by eye (c.f. Mertsch & Sarkar 2013 prediction)



Spectral indices

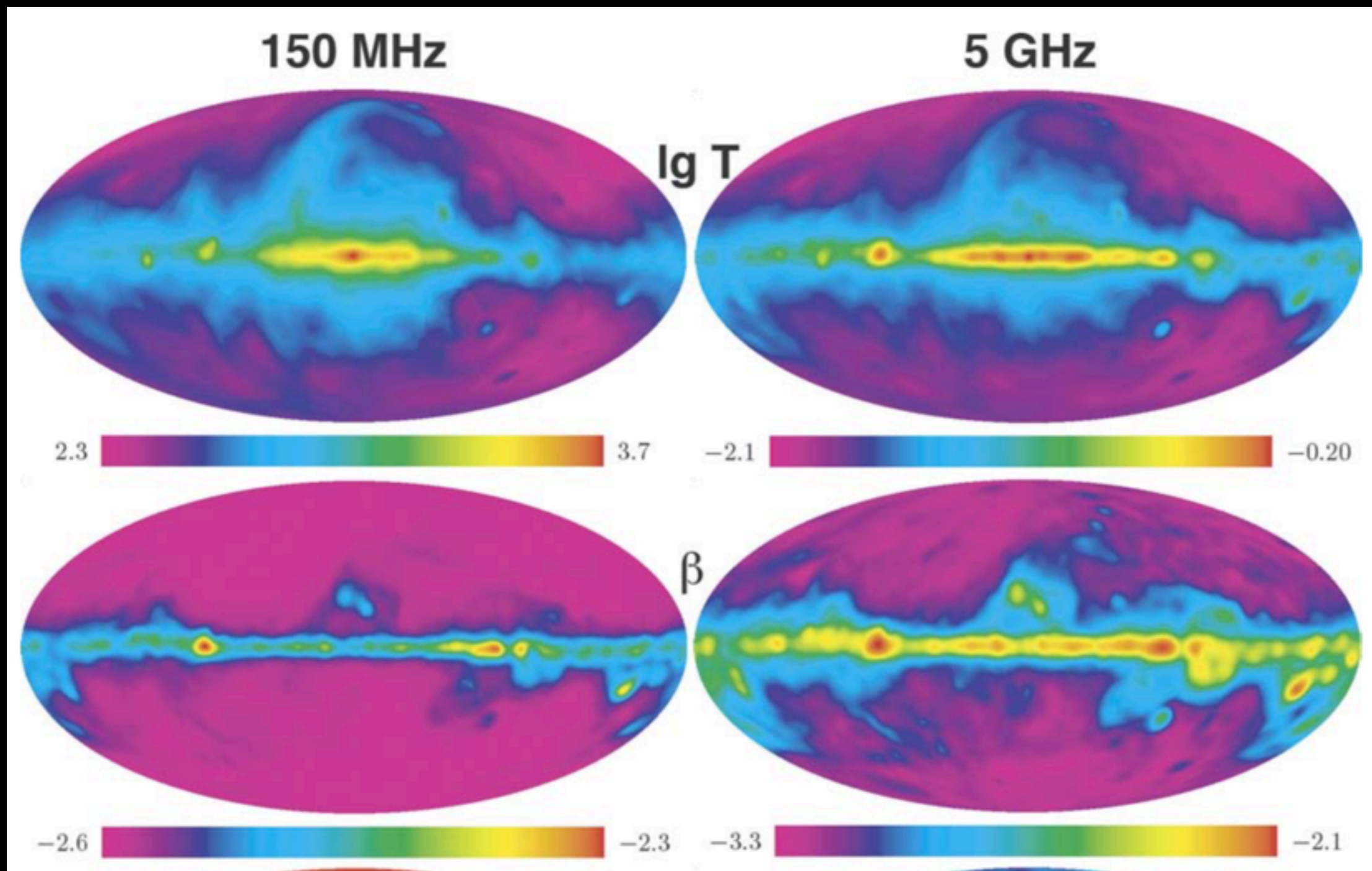
Synchrotron spectrum generally steepens with frequency (spectral ageing)

Diffuse synchrotron $\beta \sim -2.7$ at 1 GHz, steepening to ~ -3.0 at 10-50 GHz (c.f. Orlando & Strong 2013)

Also steeper towards the plane due to star formation

Spurs: typically steep (-3.0) across wide-range of frequencies

(suggests older electrons, no new power source)



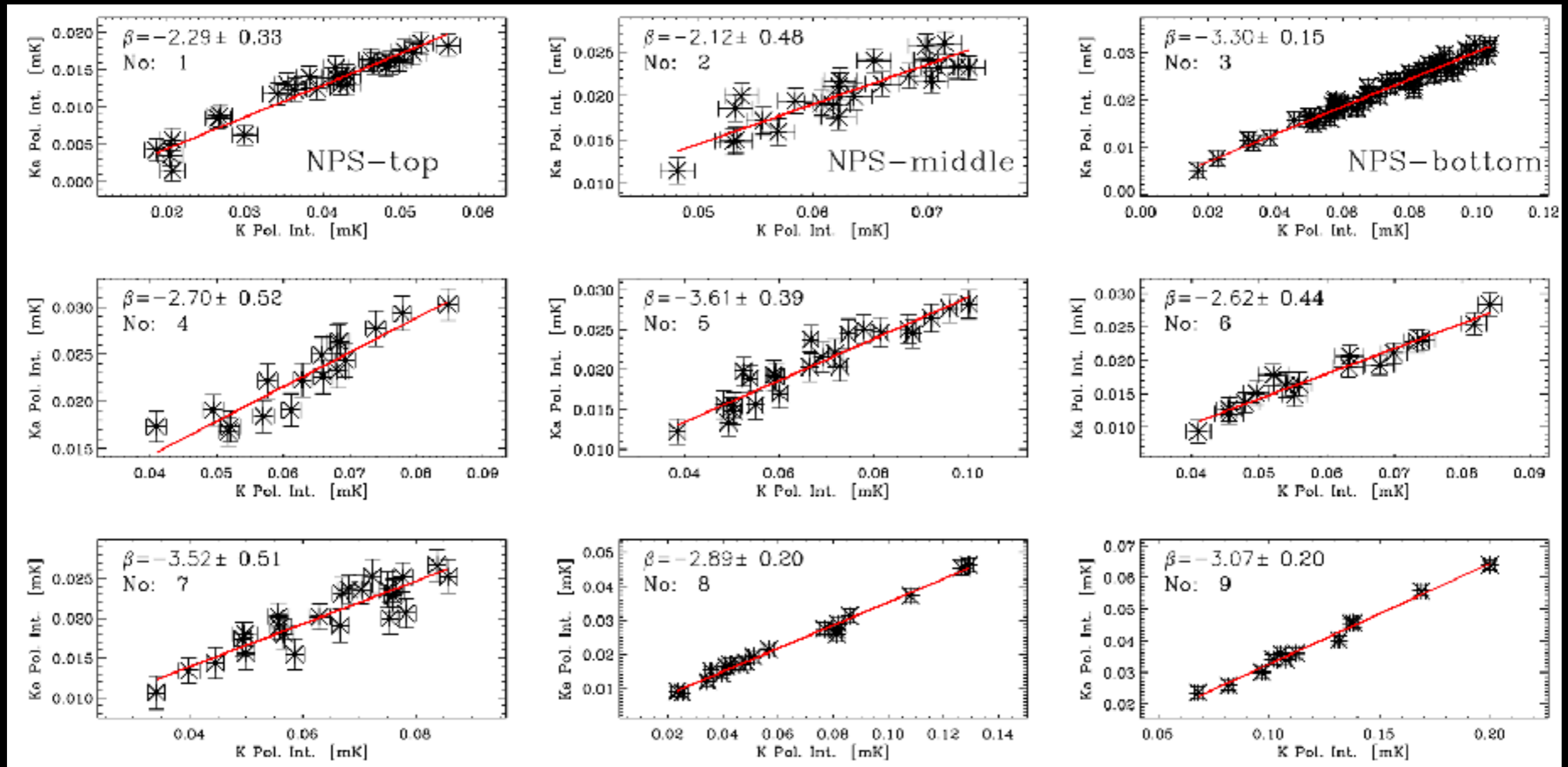
Spectral indices

Dickinson et al. (2009)

Intensity complicated due to component separation
Polarization easier but noisier!
(noisy data & frequencies close together)

T-T plots not affected by zero levels!

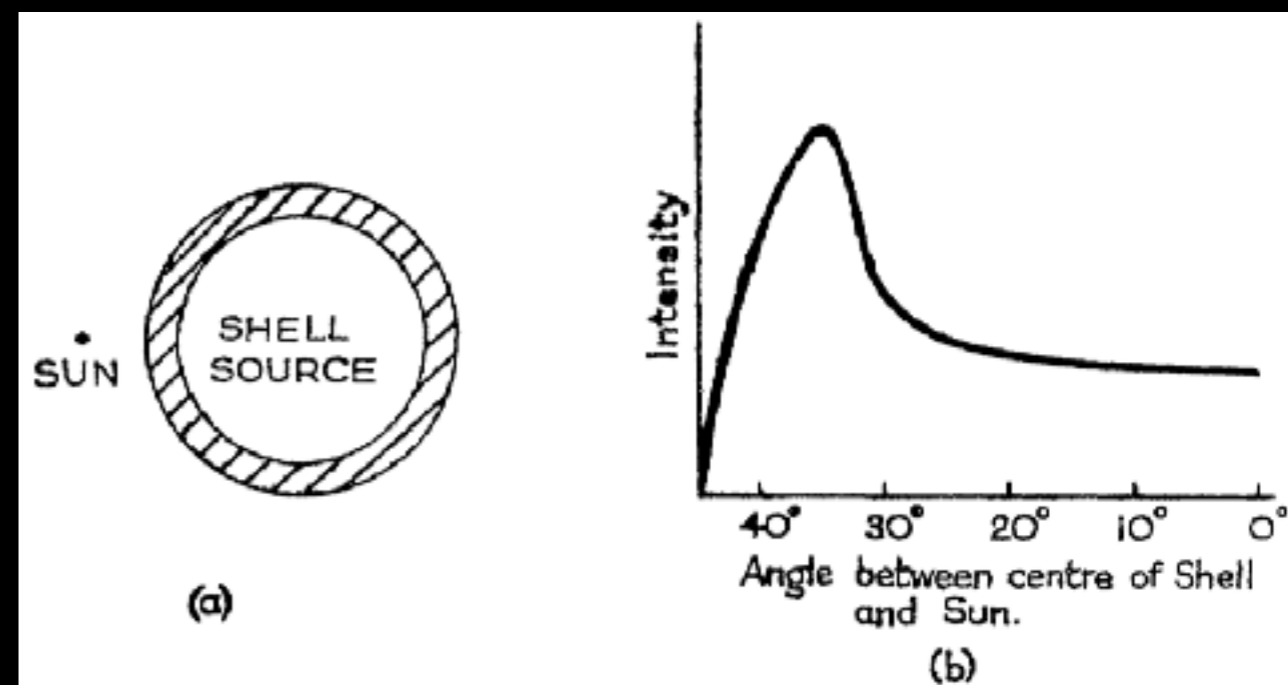
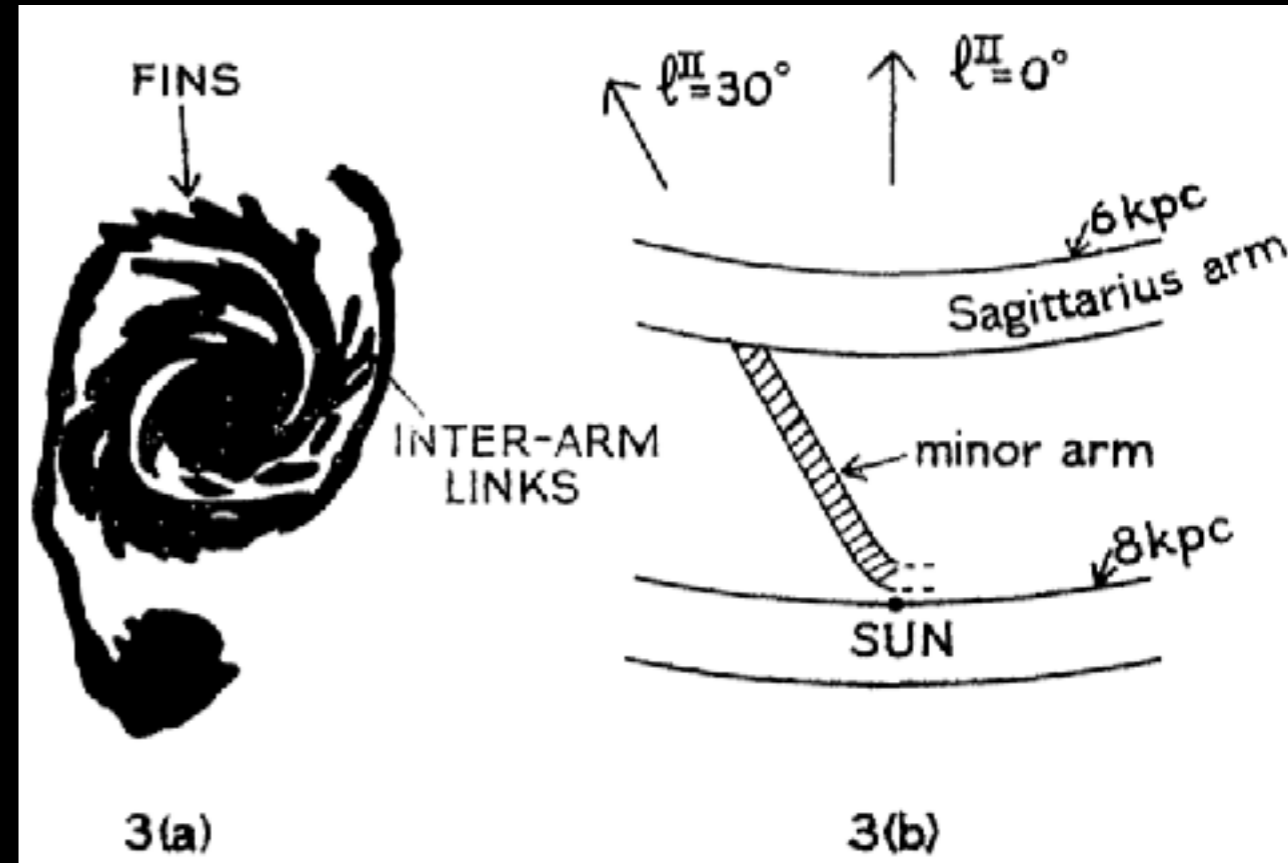
Frequency Range	Reference	$\beta \pm \Delta\beta$ ($ b > 20^\circ$)
0.408–2.3 GHz	D. P. Finkbeiner (2009, private comm.)	-2.69 ± 0.12
0.408–2.3 GHz	Giardino et al. (2002)	-2.90 ± 0.06
0.408–2.3 GHz	Platania et al. (2003)	-2.68 ± 0.11
23–94 GHz	Gold et al. (2009)	-3.18 ± 0.17
0.408–23 GHz	G. Giardino (2009, private comm.)	-2.89 ± 0.13
23–94 GHz	This paper	-2.97 ± 0.21



Vidal et al. (2015)

Many early theories... (e.g. Berkhuijsen et al. 1971, Salter 1983)

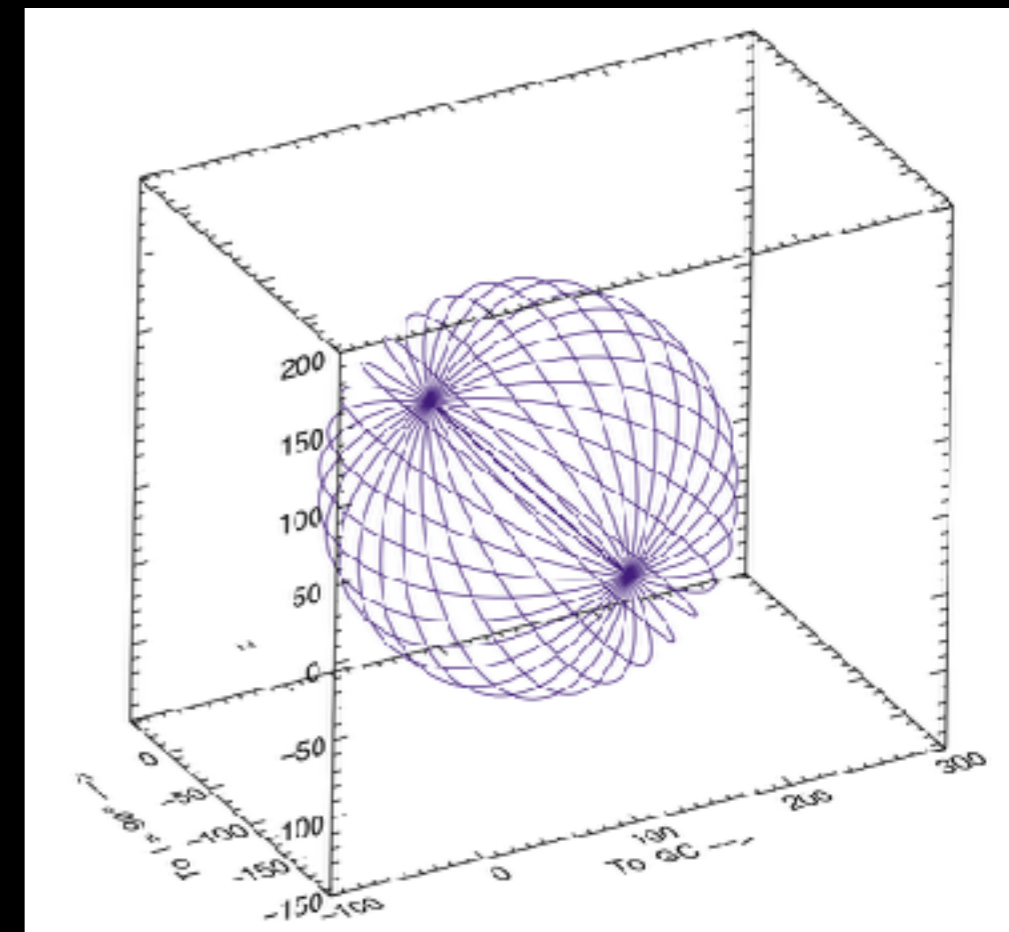
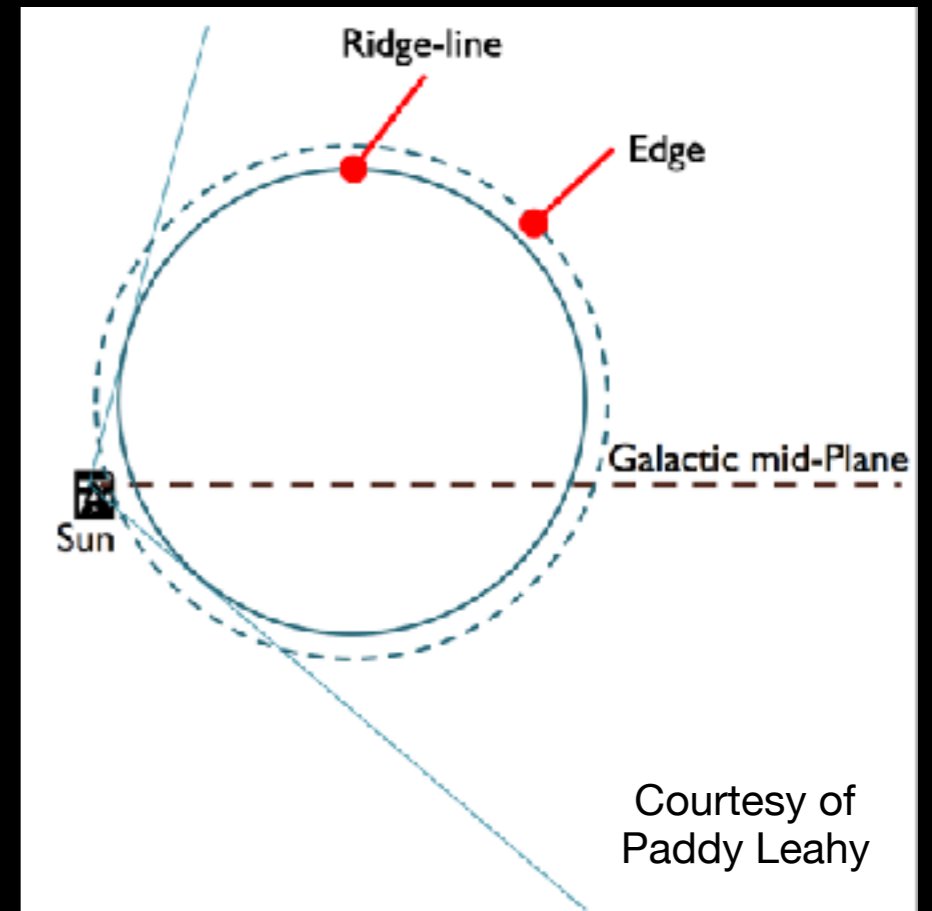
- Remnants: Type I/II supernova outbursts
- Remnants: “Super” supernova outbursts
- Joins across Galactic plane to form helical structure
- Radio tracers of helical local Galactic magnetic field
- Bubbles/loops in local magnetic field
- Stellar winds from Scorpio-Centaurus OB association
- Hypershell of starburst activity, possibly near the Galactic centre
- Minor spiral arms
- Fossilised Stromgren spheres
-



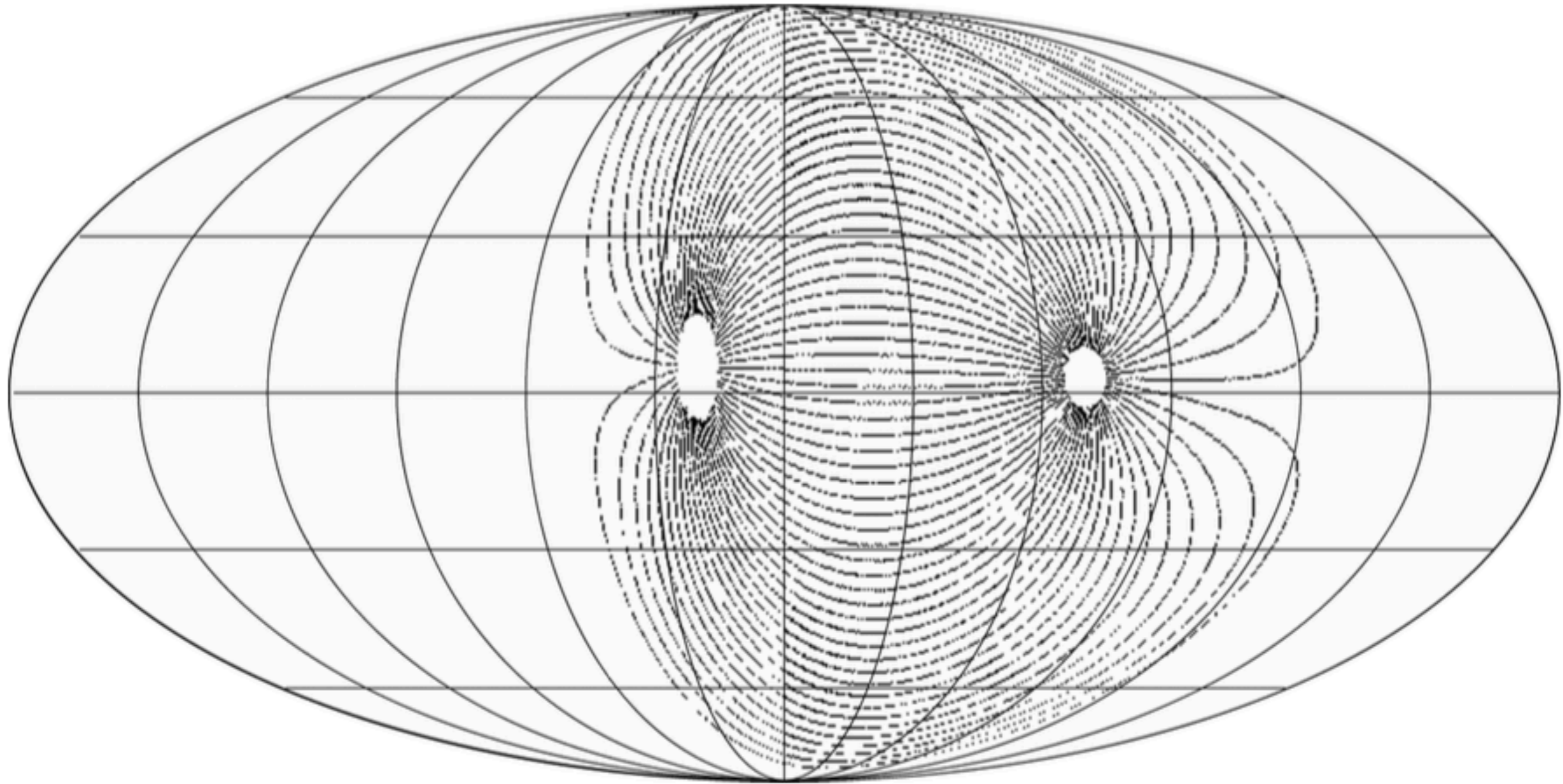
Brown et al. (1960)

A proposed model for Loop I (Heiles et al. 1998)

- Assume B-field parallel to plane near Sun
- Expanding supershell will bend B-field lines following lines of constant longitude
- Observed pattern less trivial - critically depends on viewing angle!
- Heiles (1998) applied this to star-light absorption data
- We repeat using WMAP synchrotron polarization maps
 - Centre @ 120 pc towards Sco-Cen association
(l,b)=(320,5)
 - Radius = 120 pc

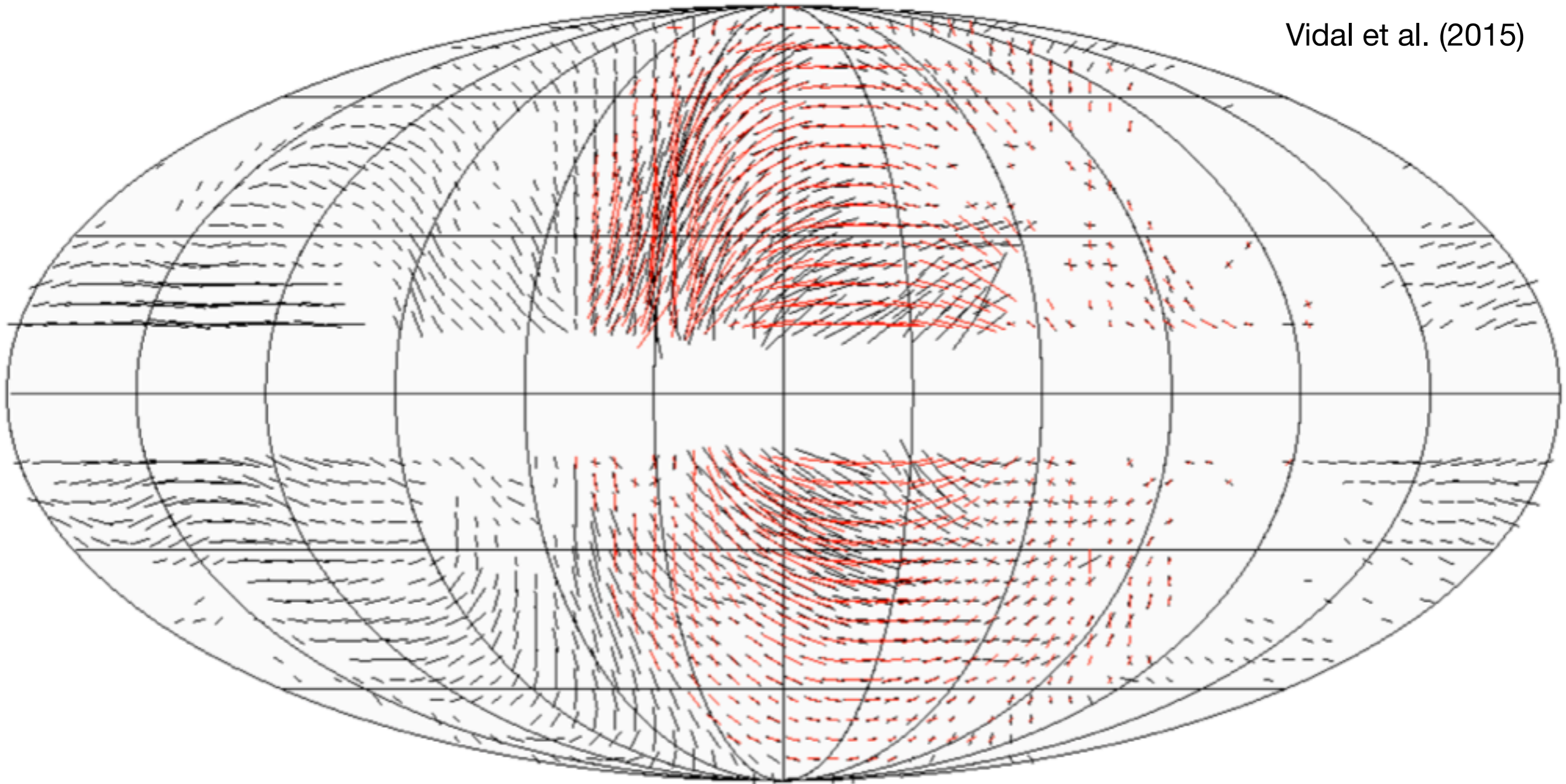


Proposed model - projection of B-field on the sky

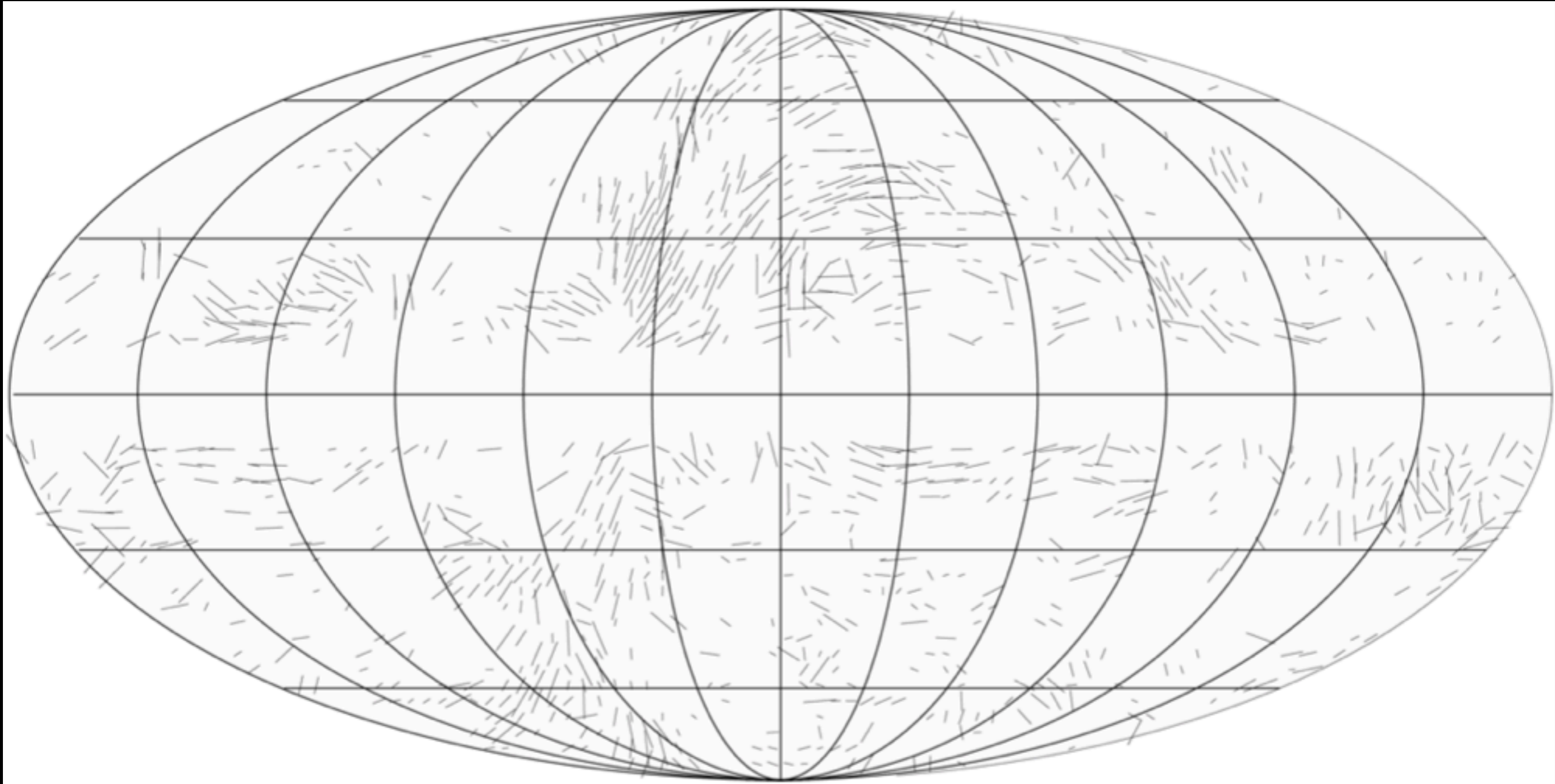


Data vs Model - good agreement!

Vidal et al. (2015)



Data vs Model - good agreement!

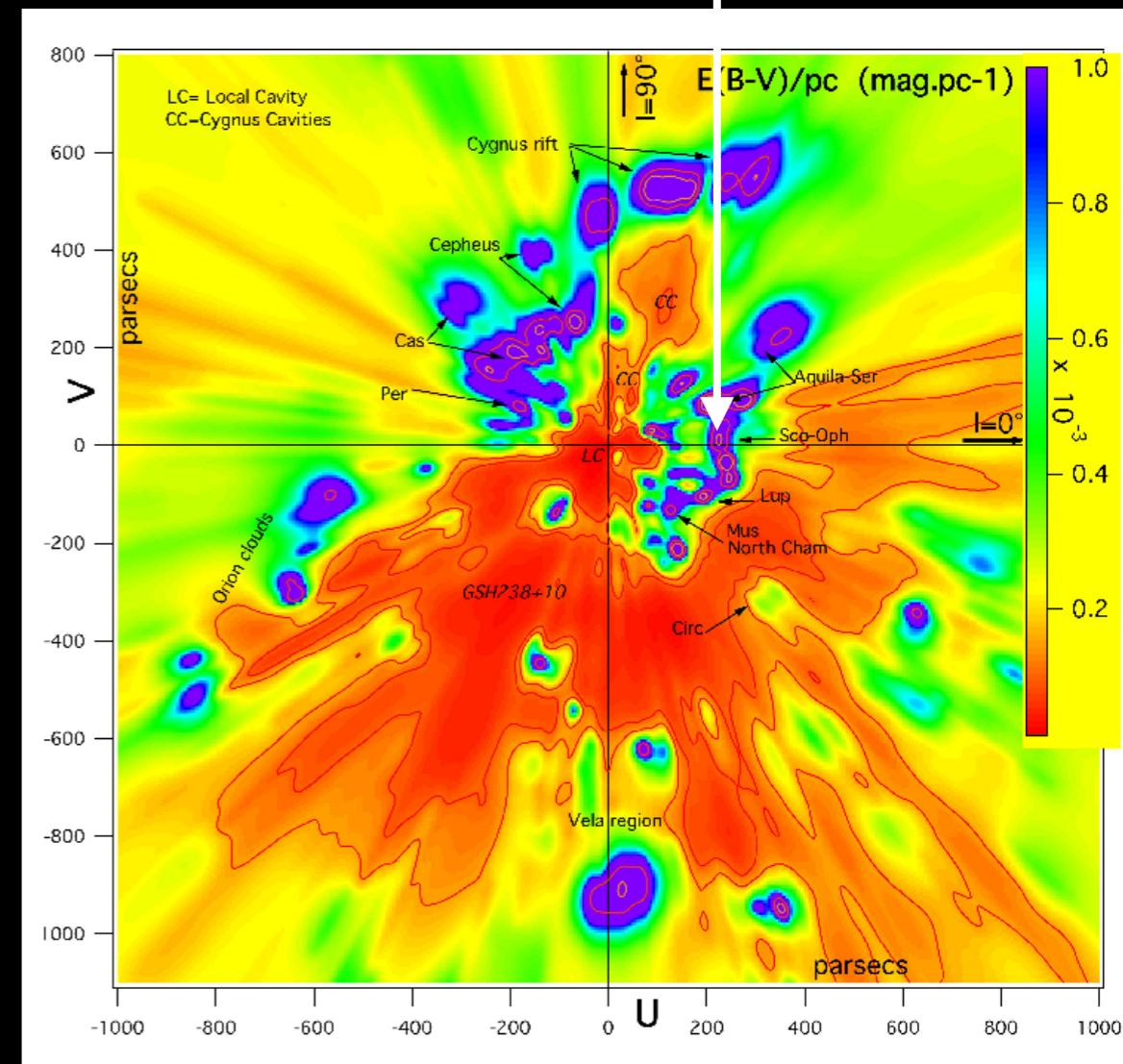


Star-light absorption (<300 pc only!)

A few comments on Loop I

- Expanding shell(s) generally appealing
 - Geometry, fit to small circles, cold HI/dust border to the outside, some emission inside etc.
 - Spurs are bundles of field lines with enhanced CR density
- Remarkably good fit to polarization directions
 - Also star-light absorption - nearby structure (<300 pc)
 - B-field outside of NPS consistent and local ISM
- Only see strong emission from part of shell?
 - Different ISM densities on either side
 - NPS close to denser Ophiuchi clouds while rest expanding into low density cavity
- Many models probably ruled out already, e.g.,
 - Bland-Hawthorn (2013) - spectral indices too steep for thermal/flat synchrotron
 - Jones et al. (2012) suggested toroidal field - error in use of WMAP Q, U maps (“cosmological” convention - not IAU, so $U=-U$!)

Wall of gas at bottom of spur at 130 pc
(Iwan et al. 1980)



3-D mapping of local ISM
Lallement et al. (2014)

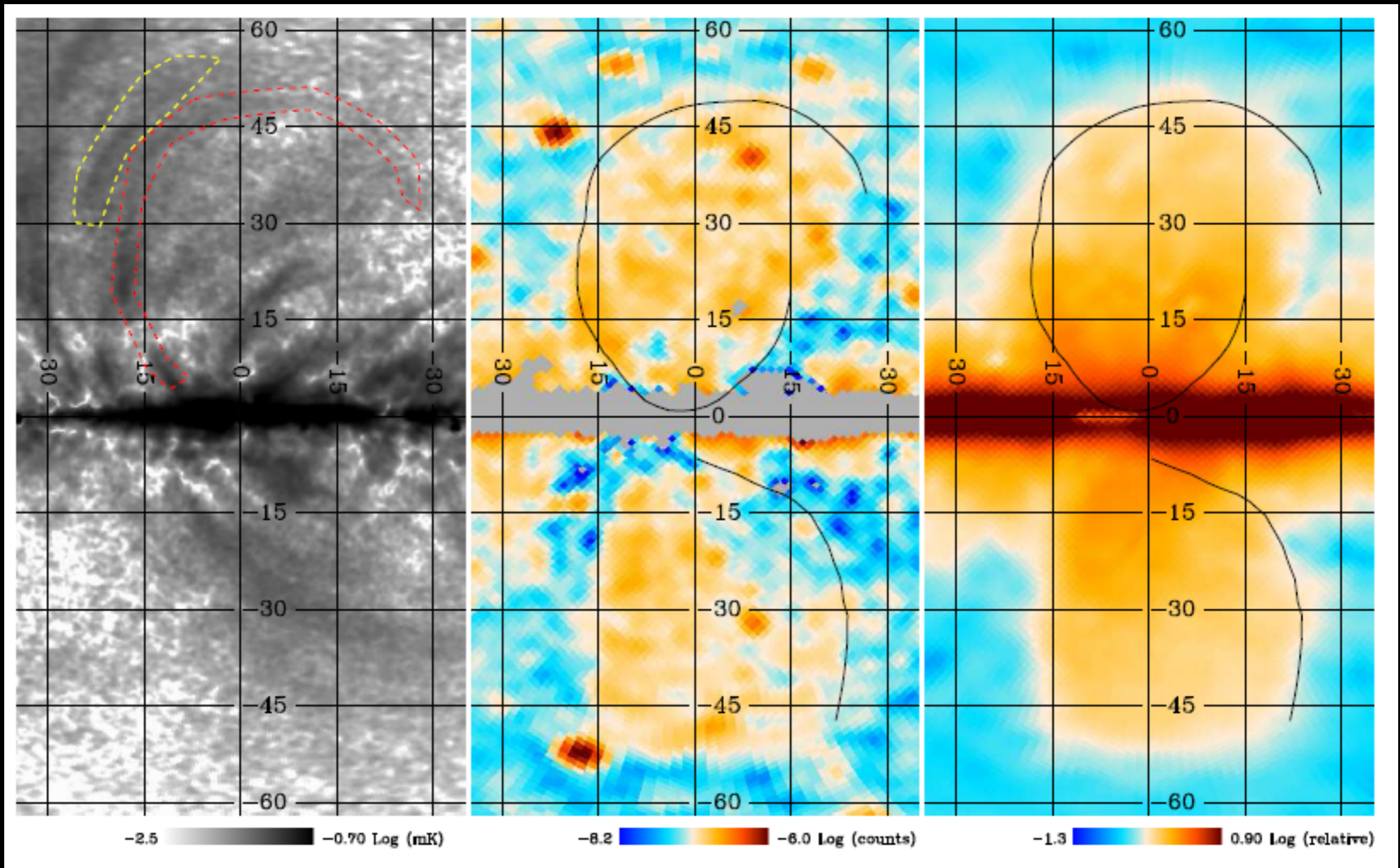
Further comments on distance

- 1. Centre of Loop is nowhere near the Galactic centre (10s of degrees)
- 2. NPS nowhere near the Galactic centre (20 deg off)
- 3. Starlight polarized absorption detects NPS beyond 100 pc (Matthewson+Ford 1970, Santos et al. 2011)
 - Also simple B field model only works well for stars <300 pc
- 4. Bright edge of NPS/Loop I roughly where dense gas exists and low density in other directions (up to ~kpc)
- 5. B-field outside of NPS consistent with local origin (coincidence? or another spur?)
- 6. Energetics (10^{55} erg) and huge size! (~7 kpc)
- 7. Southern part of FB extends outside Loop I and no trace of interaction with FB in radio maps
- 8. Loop I extends through the Galactic plane without any sign of deviation
- 9. We see lots of other loops/spurs with similar geometry, spectral index etc.
- [Sofue et al. (2015) arguments not all sound e.g. Aquila rift not at a single distance]
- **My conclusion: Models putting loop I at Galactic centre (e.g. Sofue et al. 1977) unlikely**
 - **However, there is some evidence that NPS/Loop I further than originally thought (~100-200pc), possibly up to ~kpc**

Fermi bubbles

Planck Collaboration XXV (2015)

Filament traces FB remarkably well - this is NOT the NPS! (inside it)
Unlikely to be related to Loop I (offset, extends outside bubble, distance etc.)
Synchrotron spectral index relatively flatter than elsewhere (~ -2.5) - unlike Loop I etc.



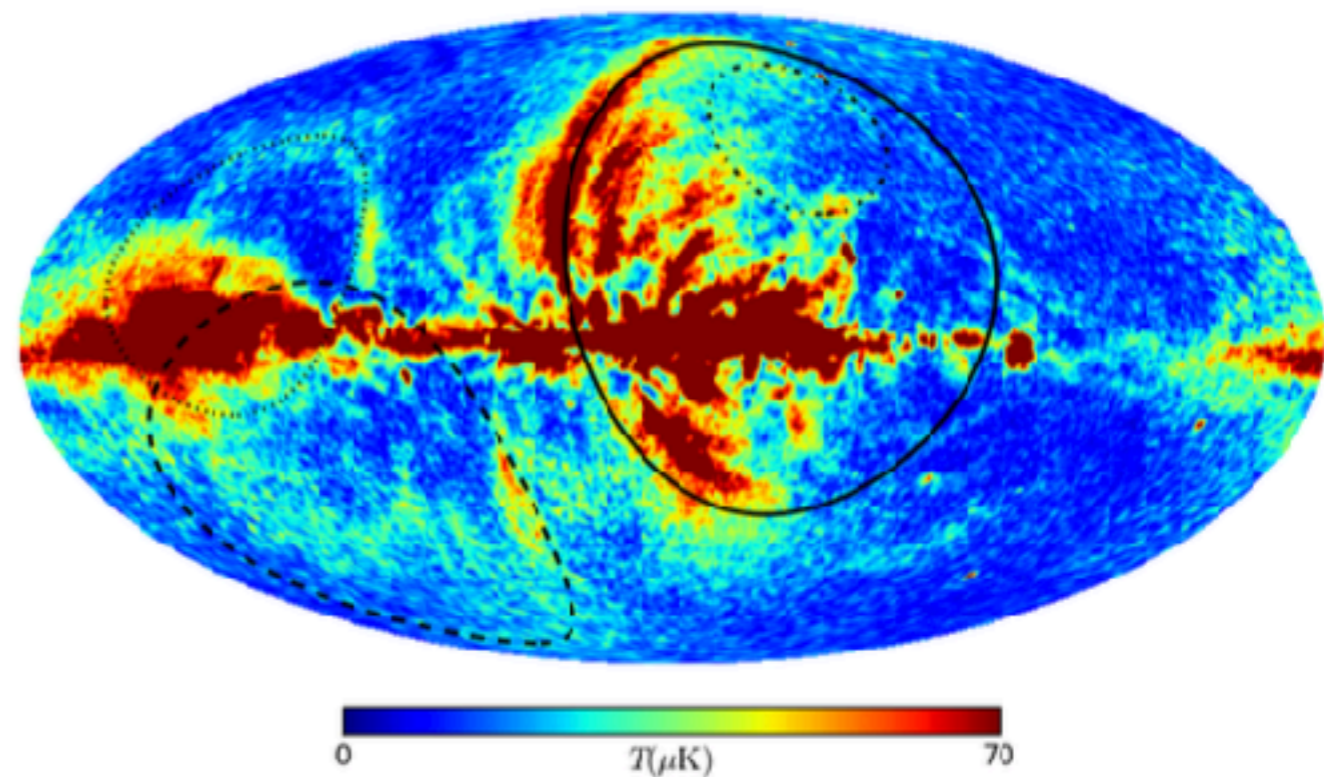
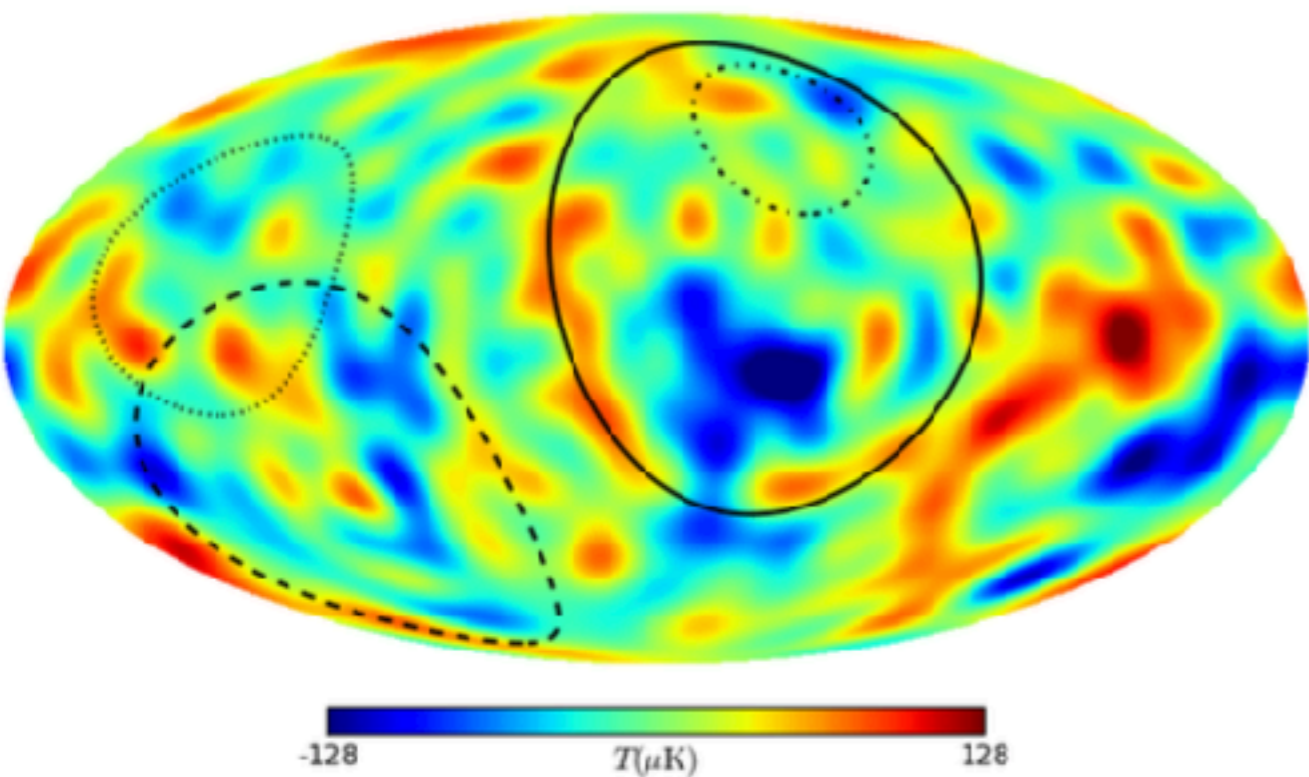
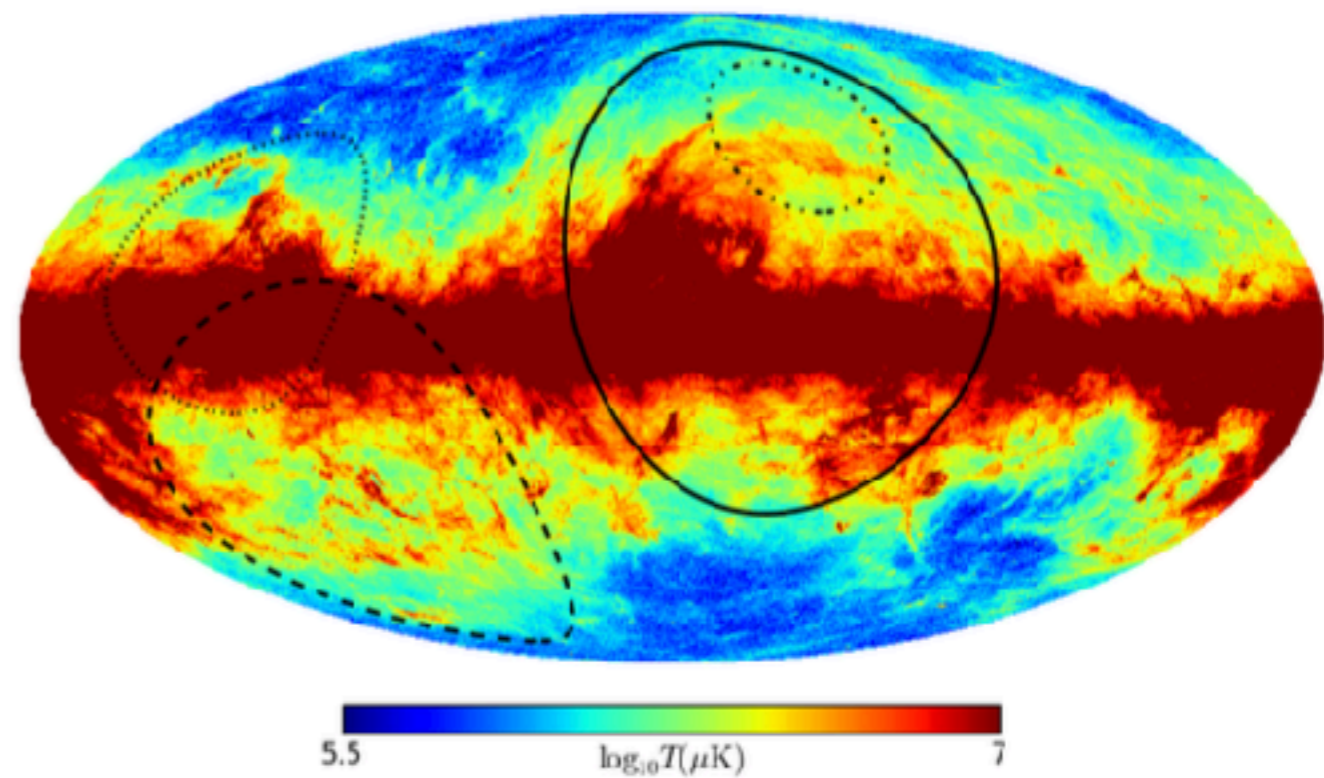
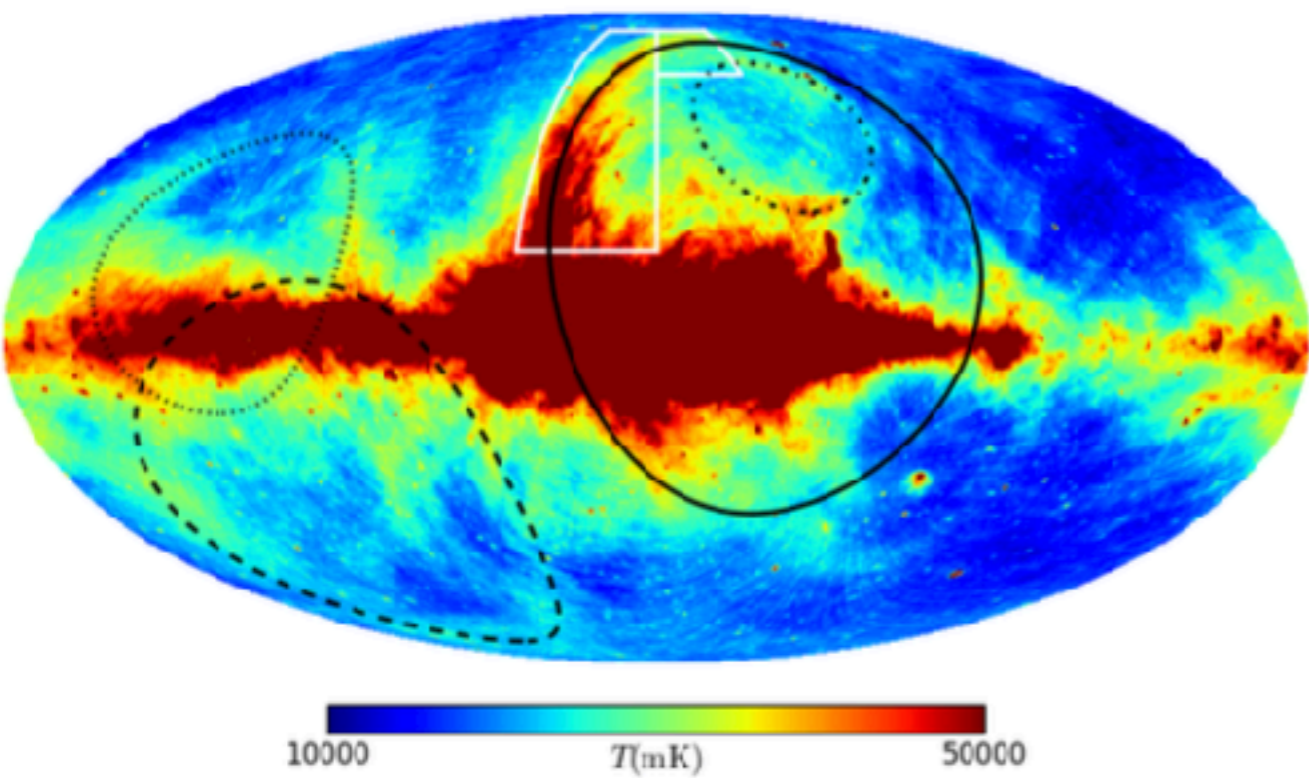
Polarized synchrotron intensity

10-500 GeV Fermi map
Corrected for π^0 decay

Fermi data processed by
Selig et al. (2014)

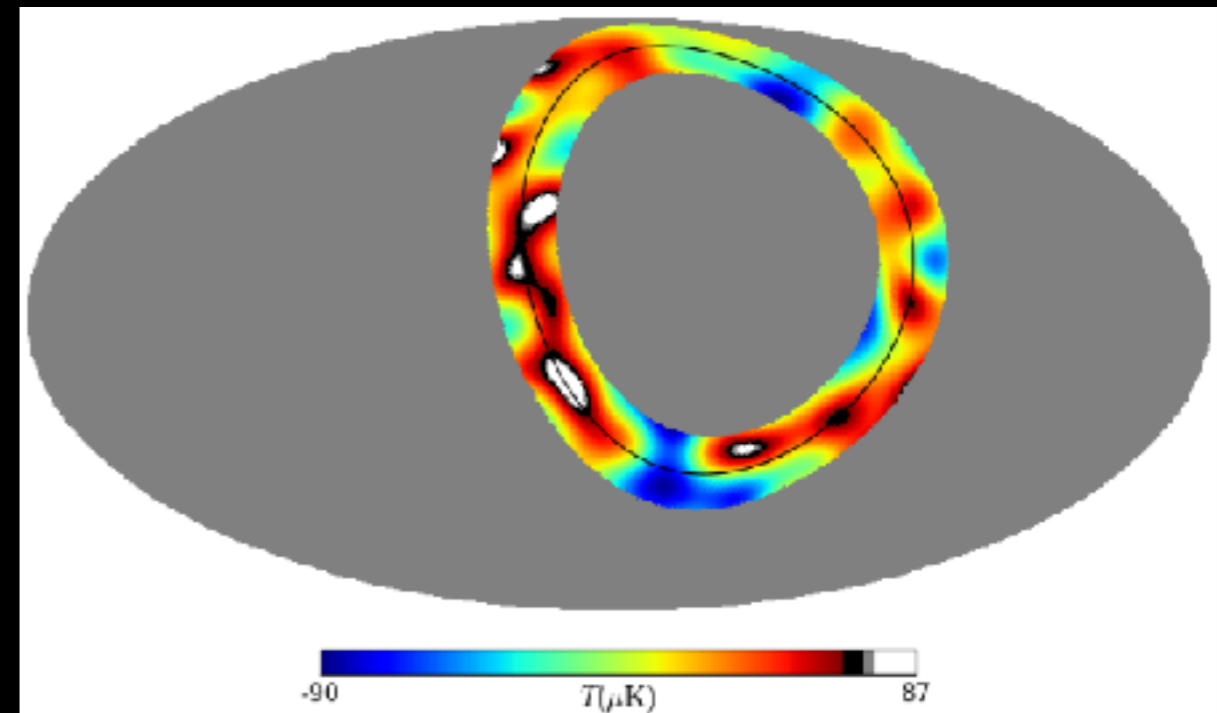
CMB contamination by loop I?

Liu et al. (2014) and von Hausegger et al. (2015)

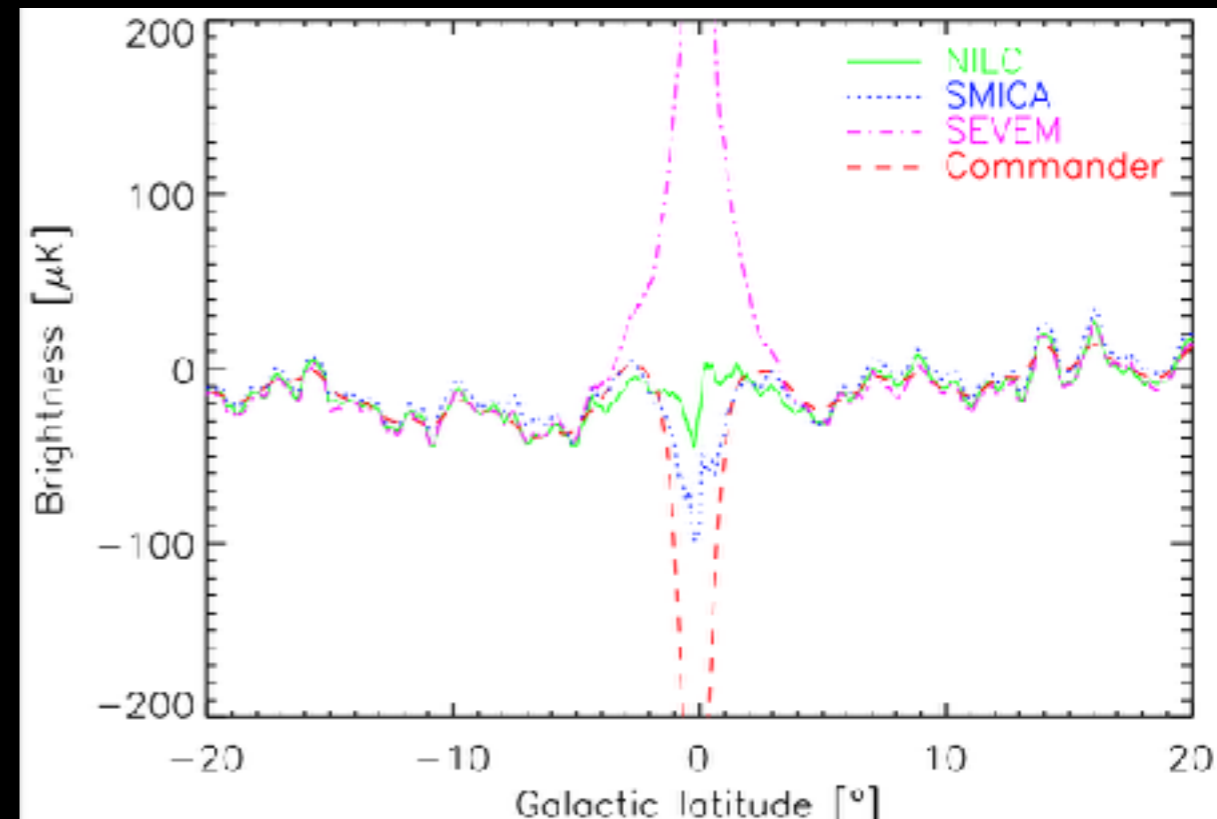


CMB contamination by loop I?

- Possible contamination from gas/dust associated with loop I (Liu et al. 2014; von Hausegger et al. 2015)
 - Magnetic dipole radiation from magnetised dust grains?
- However, note that:
 - Statistics difficult to quantify due to “look elsewhere effect” (e.g. trial factors)
 - Alignment is not actually very good with dust which is exterior to loop I (only with theoretical outline)
 - Peaks of CMB $\sim 10\times$ estimated errors by WMAP and Planck teams
 - Also, peaks tend to be close to recommended Galactic masks
 - Would expect much more emission from other loops at lower latitudes



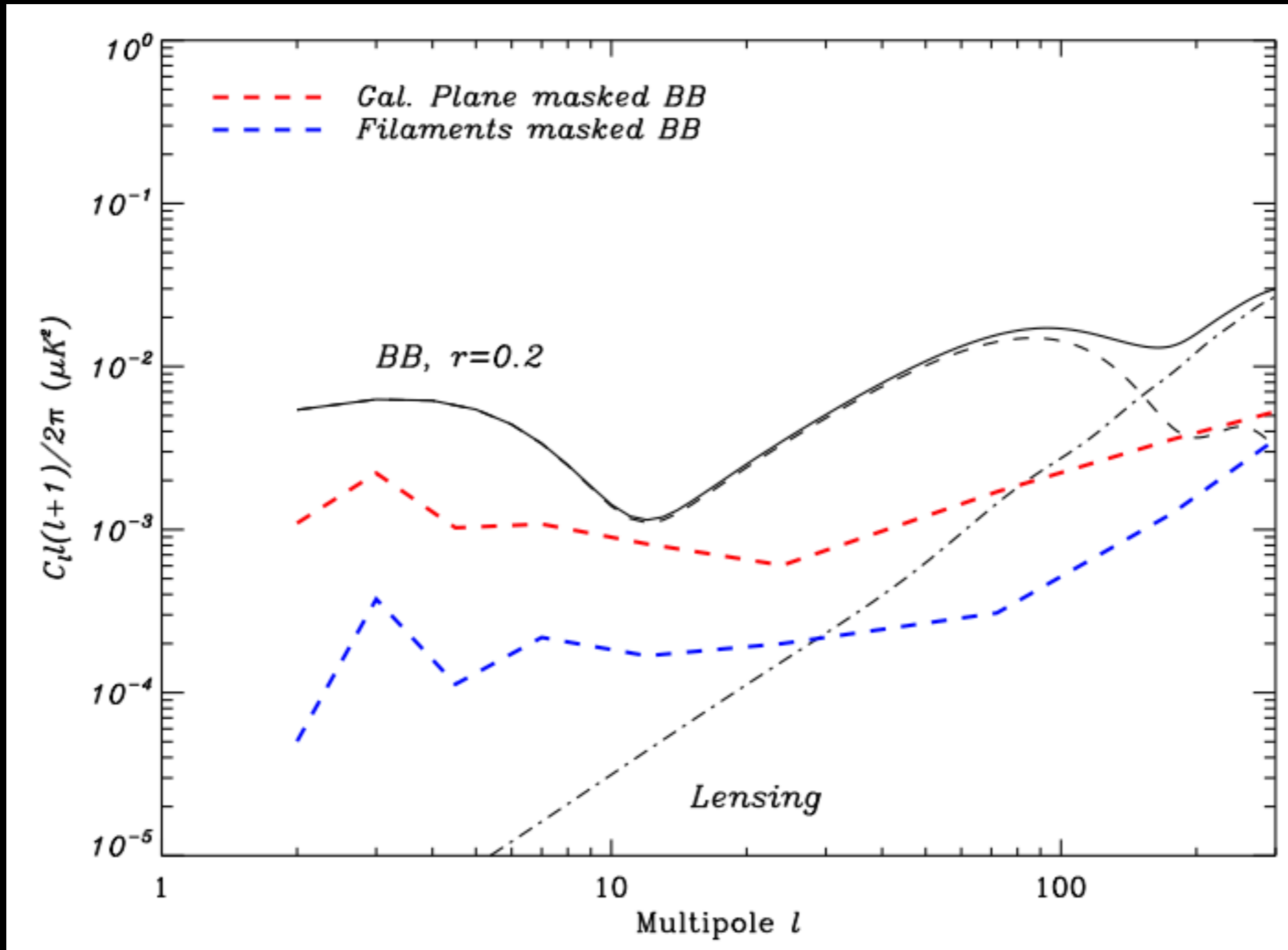
Liu et al. (2014)



CMB polarization contamination by loops

Main loops account for majority of the polarized synchrotron foreground on large angular scales
(very important for sensitive B-mode searches, especially if $r < 0.01$)

Current limit $r < 0.06$ (!)

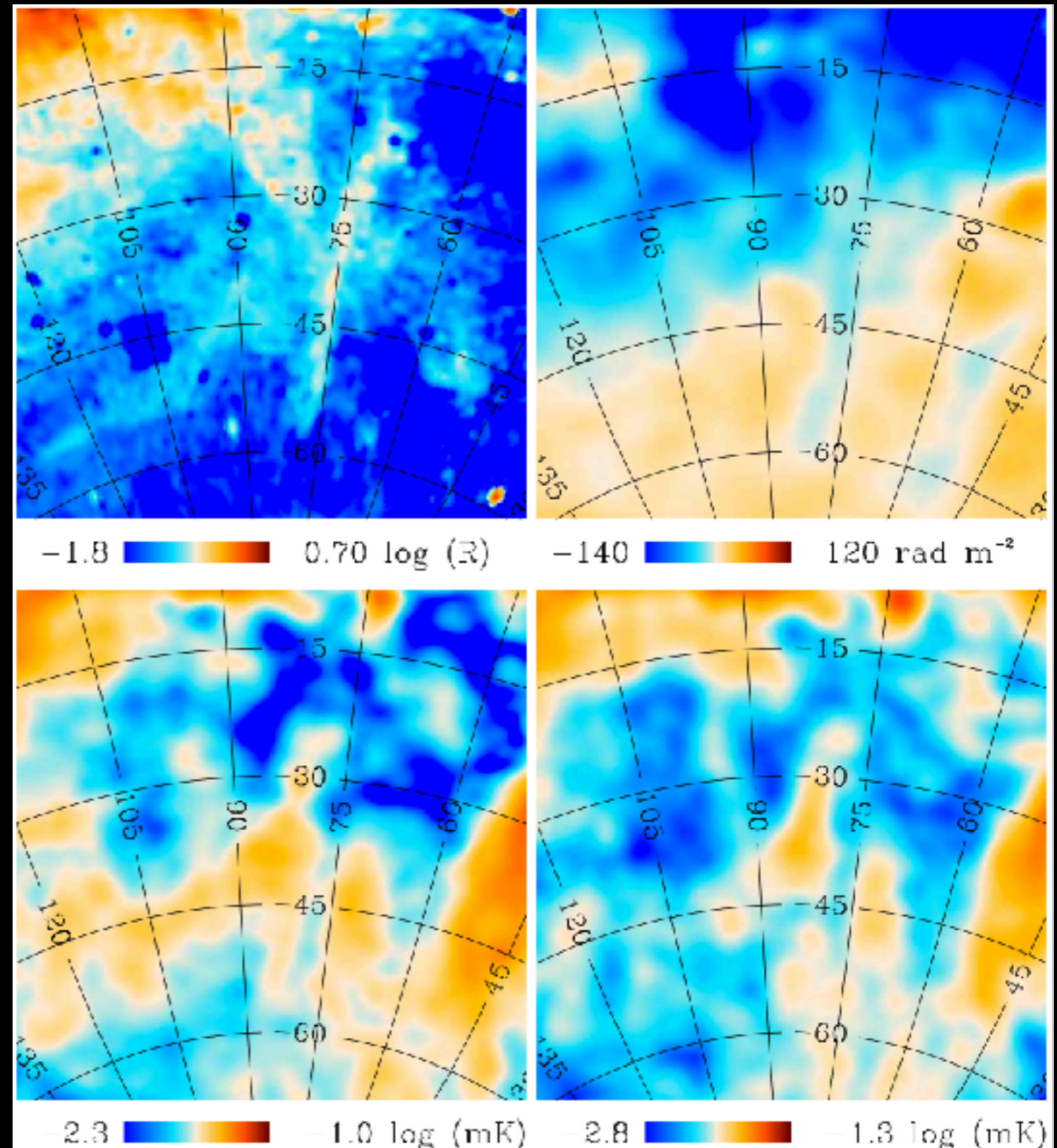


Halpha-polarized synchrotron anti-correlation

- Discovered trough in polarized synchrotron intensity at 23+ GHz where lies a narrow 40 deg H-alpha filament
 - Other places in the sky also show this on a range of scales
- Also visible in Faraday Depth map

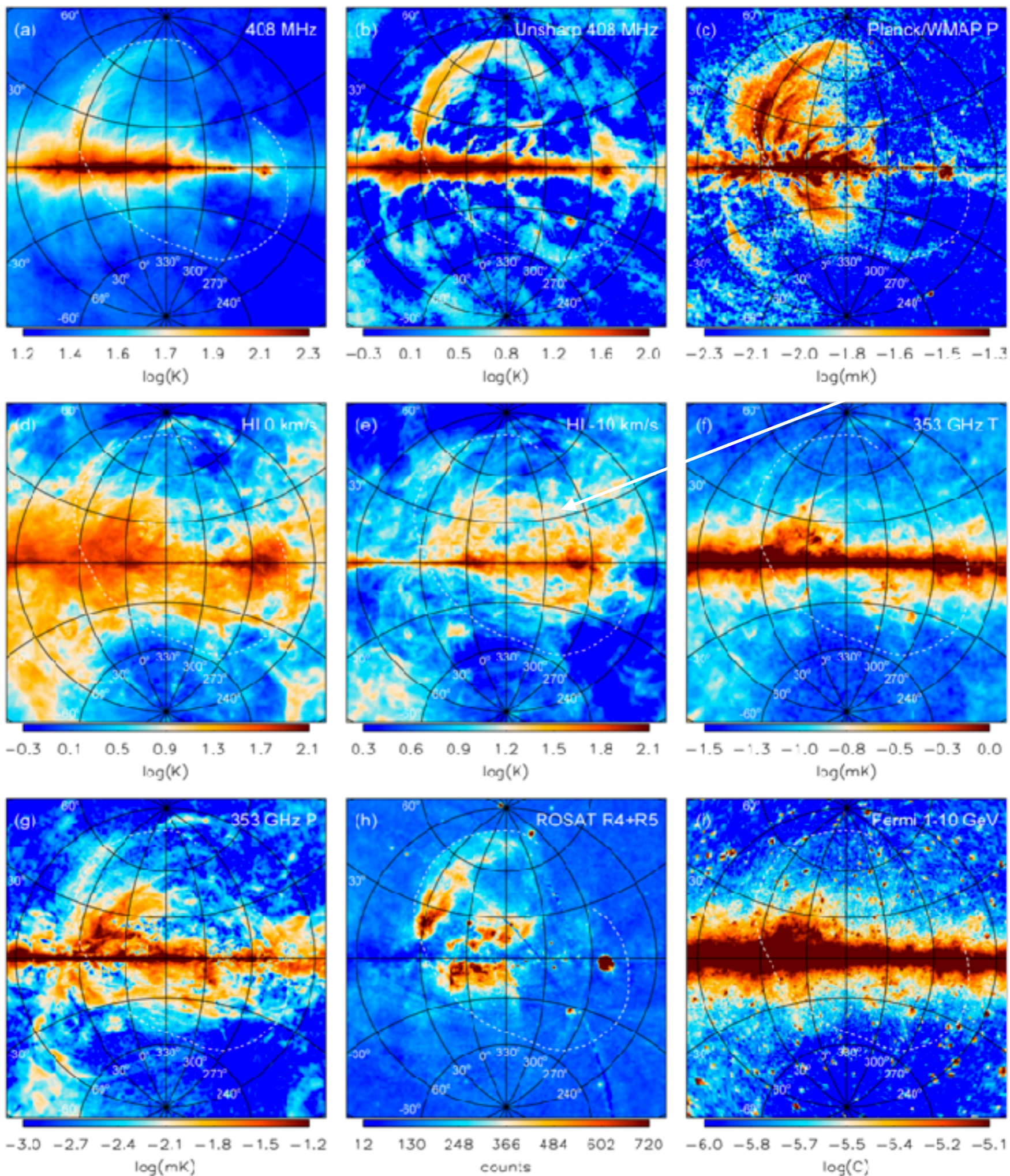
$$\phi = k_F \int_{r_0}^0 dr n_e(r) B_r(r).$$

- $\Phi = -25 \text{ rad/m}^2$
- Not a chance correlation
- Very unlikely be due to Faraday depolarization (expect < 1 deg rotation at 23 GHz for $B < 30 \mu\text{G}$)
- Possibly strong coherent B field parallel to line-of-sight of filament (cancellation)
- Synchrotron emission from ionized region intrinsically weakly polarized



Conclusions

- New data are giving a (slightly!) clearer picture of large-scale radio emission
 - Polarization data above a few GHz provide projected B-field directions
- Loops I-IV clearly visible along with several other filaments/spurs
 - Steep spectrum ($\beta \sim -3.0$) from “older” synchrotron radiation
 - Highly polarized ($\sim 30-40\%$) - highly ordered B-field
 - B-field aligned close to edge of ridges - compression due to expansion
 - Most are very nearby ($< \text{kpc}$)
- Simple expanding shell model can reproduce distribution of polarization angles
 - Only see one side due to different densities in the ISM?
- Sensitive CMB polarization measurements will need to be careful!
 - Foreground contamination dominated by large-scale spurs & filaments!
 - Also Galactic B-field modelling hopeless without taking them into account (with distances!)
- Fermi bubbles probably not related to Loop I which is probably $< \text{kpc}$ away
 - One or two of the other spurs (NPS?) might be though!



Sco-Cen supershell
(centred 120 pc away)